

The Supersymmetric Fine-Tuning Problem and TeV-Scale Exotic Scalars

Yasunori Nomura and Brock Tweedie

Department of Physics, University of California, Berkeley, CA 94720

Theoretical Physics Group, Lawrence Berkeley National Laboratory, Berkeley, CA 94720

Abstract

A general framework is presented for supersymmetric theories that do not suffer from fine-tuning in electroweak symmetry breaking. Supersymmetry is dynamically broken at a scale $\Lambda \approx (10 \sim 100)$ TeV, which is transmitted to the supersymmetric standard model sector through standard model gauge interactions. The dynamical supersymmetry breaking sector possesses an approximate global $SU(5)$ symmetry, whose $SU(3) \times SU(2) \times U(1)$ subgroup is explicitly gauged and identified as the standard model gauge group. This $SU(5)$ symmetry is dynamically broken at the scale Λ , leading to pseudo-Goldstone boson states, which we call xyons. We perform a detailed estimate for the xyon mass and find that it is naturally in the multi-TeV region. We study general properties of xyons, including their lifetime, and study their collider signatures. A generic signature is highly ionizing tracks caused by stable charged bound states of xyons, which may be observed at the LHC. We also consider cosmology in our scenario and find that a consistent picture can be obtained. Our framework is general and does not depend on the detailed structure of the Higgs sector, nor on the mechanism of gaugino mass generation.

1 Introduction

Weak-scale supersymmetry has long been the leading candidate for physics beyond the standard model. It stabilizes the Higgs potential against potentially huge radiative corrections, giving a consistent theory of electroweak symmetry breaking. Combined with the idea of dynamical supersymmetry breaking (DSB), a large hierarchy between the weak and the Planck scales is explained by a dimensional transmutation associated with DSB gauge interactions [1]. The framework also leads to an elegant picture of gauge coupling unification at a scale of $M_X \simeq 10^{16}$ GeV [2]. In addition, weak-scale supersymmetry has a virtue that it is relatively easier to evade constraints from precision electroweak measurements, compared with other candidates for physics beyond the standard model.

Despite these impressive successes, the most naive supersymmetric extension of the standard model suffers from problems. First of all, generic superparticle masses of order the weak scale lead to too large flavor changing neutral currents. This requires some organizing principle for the spectrum of superparticles. The most promising one is “universality” — the superparticles having the same standard model gauge quantum numbers are highly degenerate in mass. With this spectrum, contributions to flavor changing neutral currents from superparticle loops are canceled to high degree, evading severe experimental constraints. Another problem comes from the fact that LEP II did not discover any superparticles or the Higgs boson. In most supersymmetric theories, this leads to severe fine-tuning of order a few percent to reproduce the correct scale for electroweak symmetry breaking. This problem is called the supersymmetric fine-tuning problem.

In this paper we first present a general discussion on how to evade the above problems of generic supersymmetric theories while preserving their successful features. We find that, requiring the absence of fine-tuning in electroweak symmetry breaking, the naturalness upperbound on the squark masses are at around (660~850) GeV quite independently of the details of the Higgs sector. The upperbound on the slepton masses is similarly given at about (310 ~ 400) GeV. We then argue that consideration along these lines naturally leads to a class of theories which predicts the existence of exotic scalar particles with mass in the multi-TeV region. In these theories the DSB sector possesses a global “unified” symmetry, of which the $SU(3) \times SU(2) \times U(1)$ subgroup is explicitly gauged and identified as the standard model gauge group. The DSB sector spontaneously breaks this global symmetry, as well as supersymmetry, at a dynamical scale of (10 ~ 100) TeV. The exotic scalar particles then arise as composite pseudo-Goldstone bosons in the DSB sector and have the same gauge quantum numbers as those of grand unified gauge bosons — $(\mathbf{3}, \mathbf{2})_{-5/6}$ in the simplest case. We call these particles *xyons*.

The scenario we consider leads to certain characteristic features for the superparticle spec-

trum, and we illustrate them by presenting the supersymmetry breaking masses for the gauginos, squarks and sleptons at a representative set of parameter points. We also estimate the mass of xyons in generic situations, using naive scaling arguments, and calculate it in terms of fundamental parameters in a class of calculable theories formulated in holographic higher dimensional spacetime. We find that the mass of xyons is naturally in the multi-TeV region, so that it is within the reach of the LHC in some of the parameter region and that the discovery potential of xyons at the Very Large Hadron Collider (VLHC) is very high. We discuss general properties of xyons, especially their lifetime, and find that they generically lead to a distinctive signature of stable massive charged particles. We also discuss other experimental signatures as well as cosmology in our scenario.

The organization of the paper is as follows. In the next section we discuss the supersymmetric fine-tuning problem and present a general argument connecting the naturalness of electroweak symmetry breaking with certain properties of the supersymmetry breaking sector. We then present our explicit framework in section 3 and study its general consequences in section 4. In particular, we study properties of xyons both in the context of generic 4D theories and the holographic theories in 5D which were constructed earlier in Ref. [3]. We also discuss experimental signals and cosmology of our scenario in section 5. Finally, in section 6 we discuss the generality of our framework, particularly emphasizing that the framework is independent of the details of the Higgs sector or the mechanism of gaugino mass generation — for example, our argument does not depend on whether the gaugino masses are Majorana or Dirac type.

2 The Supersymmetric Fine-Tuning Problem

Our argument starts from carefully identifying the sources of the supersymmetric fine-tuning problem. A part of this argument also appears in [4]. In the minimal supersymmetric standard model (MSSM), the minimization of the tree-level Higgs potential gives the equation $M_Z^2/2 \simeq -m_h^2 - |\mu|^2$, where m_h^2 is the soft supersymmetry-breaking mass squared for the up-type Higgs boson and μ the supersymmetric mass for the two Higgs doublets. The Z -boson mass, M_Z , appears on the left-hand-side because the quartic coupling of the MSSM Higgs potential is given by $\lambda = (g^2 + g'^2)/8$ at tree level. This relation is in general violated at radiative level, or if we extend the Higgs sector such that there are additional sources for the Higgs quartic coupling. In these cases the above equation is modified to

$$\frac{M_{\text{Higgs}}^2}{2} \simeq -m_h^2 - |\mu|^2, \quad (1)$$

where M_{Higgs} is the mass of the physical Higgs boson. This equation is valid for moderately large values for $\tan \beta \equiv \langle h \rangle / \langle \bar{h} \rangle$, e.g. $\tan \beta \gtrsim 2$, where h and \bar{h} are the up-type and down-type Higgs

doublets, respectively. For smaller values of $\tan\beta$, correction terms of order $1/\tan^2\beta$ should be included in the right-hand-side.¹

In the MSSM, M_{Higgs} is smaller than about 130 GeV. This implies that if we want to avoid significant fine-tuning between the two unrelated parameters m_h^2 and μ , each term in the right-hand-side of Eq. (1) cannot be much larger than about $(160 \sim 210 \text{ GeV})^2$.² The size of $|\mu|$ is constrained to be $|\mu| \gtrsim 100 \text{ GeV}$ by the chargino search, but it still allows $|\mu| \lesssim 210 \text{ GeV}$. For m_h^2 , there are several contributions to this quantity. In particular, loops of the top quark and squarks give the contribution

$$\delta m_h^2 \simeq -\frac{3y_t^2}{4\pi^2} m_{\tilde{t}}^2 \ln\left(\frac{M_{\text{mess}}}{m_{\tilde{t}}}\right), \quad (2)$$

where y_t is the top Yukawa coupling, and $m_{\tilde{t}}$ represents the masses of the two top squarks, which we have taken to be equal for simplicity. Here, M_{mess} is the scale at which superparticle masses are generated (or at which supersymmetry breaking is mediated to the supersymmetric standard model sector), which we call the messenger scale. The absence of unnatural cancellations then implies that the values of $|\delta m_h^2|$ should not be much larger than the bound on m_h^2 itself, $(160 \sim 210 \text{ GeV})^2$.

Assuming flavor universality for the squark and slepton masses, the current mass bound for the top squarks is roughly $m_{\tilde{t}} \gtrsim 300 \text{ GeV}$ [5]. Now, imagine that the messenger scale is very high, of order the Planck scale, $M_{\text{mess}} \simeq M_{\text{Pl}}$, as in the case of the minimal supergravity scenario. In this case the logarithm $\ln(M_{\text{mess}}/m_{\tilde{t}})$ is very large ($\simeq 35$), and Eq. (2) gives $-\delta m_h^2$ as large as $(500 \text{ GeV})^2$ even for $m_{\tilde{t}}^2 \simeq (300 \text{ GeV})^2$. (In fact, the value of $m_{\tilde{t}}^2$ is constrained to be even larger in conventional supersymmetric theories, see discussions below.) This, therefore, requires a severe cancellation between the two terms in Eq. (1) at a level of a few percent. In fact, because of the large logarithm, a precise analysis requires summing up the leading logarithms using renormalization group equations. However, the result is essentially unchanged, and a fine-tuning of order a few percent is still required [6]. This argument suggests that smaller values of M_{mess} are preferred from the naturalness point of view.

Suppose now that M_{mess} is small and close to the electroweak scale, $M_{\text{mess}} \simeq (10 \sim 100) \text{ TeV}$. In this case the logarithm in Eq. (2) can be quite small, and of a factor of a few. In the MSSM,

¹Appropriate correction terms are given by $\{m_h^2 - m_{\bar{h}}^2 + 2(\mu B) \tan\beta\}/(\tan^2\beta + 1)$, where μB is the holomorphic supersymmetry-breaking mass for h and \bar{h} , which is generically of order $1/\tan\beta$. Note that for small $\tan\beta$, this equation deviates from the famous relation, $M_{\text{Higgs}}^2/2 = (m_{\bar{h}}^2 - m_h^2 \tan^2\beta)/(\tan^2\beta - 1) - |\mu|^2$. Our equation is obtained by looking along the direction of the vacuum expectation value in the field space of h and \bar{h} . This is generically valid as long as the charged Higgs boson mass is somewhat larger than the lightest Higgs boson mass, M_{Higgs} , which we expect to be the case to evade the constraint from $b \rightarrow s\gamma$.

²The numbers we provide correspond to the requirement that each term in the equation determining the weak scale must not be larger than a factor $(3 \sim 5)$ times the sum of all the terms, i.e. the level of a cancellation must not be severer than $(20 \sim 33)\%$.

however, this still does not allow us to eliminate the fine-tuning. The obstacle arises essentially from the conflict between the LEP II bound on the Higgs-boson mass, $M_{\text{Higgs}} \gtrsim 114$ GeV [7], and the tree-level MSSM prediction, $M_{\text{Higgs}} \leq M_Z$, which requires a significant radiative correction to M_{Higgs} . Such a large correction arises in the MSSM only when the top squarks are heavy. For natural values of the top-squark mass parameters, the LEP II bound, $M_{\text{Higgs}} \gtrsim 114$ GeV, requires $m_{\tilde{t}}$ to be larger than about (800 ~ 1000) GeV [8]. This in turn requires cancellations among various terms in the right-hand-side of Eq. (1) at a level of (4 ~ 6)%, at best.³

A lower bound on $m_{\tilde{t}}$ can also come from the pattern of superparticle masses. For very small values of M_{mess} , the most natural mechanism giving flavor-universal superparticle masses is to mediate supersymmetry breaking through standard model gauge interactions, $SU(3)_C \times SU(2)_L \times U(1)_Y$ (321). This implies that the DSB sector, or some sector that feels the primary supersymmetry breaking, is charged under 321 gauge interactions and thus contributes to the evolution of the 321 gauge couplings above M_{mess} . This contribution, therefore, destroys the successful supersymmetric prediction for the low-energy gauge couplings unless it is somehow universal for $SU(3)_C$, $SU(2)_L$ and $U(1)_Y$.⁴ The simplest possibility to preserve the prediction is then that the DSB sector, or the corresponding sector, respects a global $SU(5)$ symmetry that contains 321 as a subgroup, so that this sector does not affect the differential evolution of the 321 gauge couplings. In this case the ratio of the top squark mass to the right-handed selectron mass is given by

$$\frac{m_{\tilde{t}}^2}{m_{\tilde{e}}^2} \simeq \frac{(4/3)g_3^4 + \delta}{(3/5)g_1^4} \simeq (7 \sim 8)^2, \quad (3)$$

where g_3 and g_1 are the $SU(3)_C$ and $U(1)_Y$ gauge couplings, renormalized at a scale of order M_{mess} , and δ represents the small contributions from $SU(2)_L$ and $U(1)_Y$.⁵ The non-discovery of the right-handed selectron at LEP II pushes up its mass to be above $\simeq 100$ GeV [5]. This leads to $m_{\tilde{t}}$ as large as, at least, 700 GeV, which in turn leads to $-\delta m_h^2$ larger than about (300 GeV)² even for $\ln(M_{\text{mess}}/m_{\tilde{t}})$ as small as a factor of a few. For $M_{\text{Higgs}} \lesssim 130$ GeV, for example, this alone requires some cancellation at a level of 10%.

³It is customary to define the amount of fine-tuning by the sensitivity of the weak scale, M_Z , to fractional changes of fundamental parameters a_i of the theory [9]: $\Delta^{-1} \equiv \min_i \{(a_i/M_Z^2)(\partial M_Z^2/\partial a_i)\}^{-1}$. In the case that supersymmetry breaking is mediated by standard model gauge interactions, a_i 's are proportional to square roots of the scalar masses squared, $a_i \propto (m_{\tilde{f}}^2)^{1/2}$, so that the fine-tuning parameter is a factor 2 smaller than the amount of cancellations quoted in the text. For the case discussed here, for example, $\Delta^{-1} \lesssim (2 \sim 3)\%$ (see e.g. [4] for details).

⁴We take the $SU(5)$ -normalization for $U(1)_Y$ throughout the paper.

⁵In fact, Eq. (3) applies to quite large classes of theories in which supersymmetry breaking is mediated by standard model gauge interactions. For example, Eq. (3) applies to the minimal model of gauge mediation [10] even if the messenger sector does not possess a global $SU(5)$ symmetry. In general, Eq. (3) applies to any gauge mediation models in which the messenger sector respects an approximate $SU(5)$ symmetry at the unification scale and in which supersymmetry breaking effects in the messenger sector are not very large.

How can we avoid this unpleasant situation? Barring a possibility of accidental cancellations, the necessary condition is to have an additional contribution to M_{Higgs} , i.e. an additional source for the Higgs quartic coupling other than the $SU(2)_L \times U(1)_Y$ D -terms in the MSSM. Such a contribution may arise, for example, from the superpotential coupling of the Higgs doublets to some other field, such as the singlet field in the next-to-minimal supersymmetric standard model (NMSSM)-type theories [11, 12, 13], or from the D -term of additional gauge interactions other than 321 of the MSSM [14, 15]. Is this sufficient to eliminate the fine-tuning? Equation (1) implies that for arbitrarily large M_{Higgs} , the naturalness requirement on the sizes of $|m_h^2|$ and $|\mu|^2$ becomes arbitrarily weaker.⁶ However, if we make M_{Higgs} very large, we lose one of the virtues of supersymmetric theories: precision electroweak constraints can be satisfied without unnatural cancellations among various contributions. If we want to keep this virtue, i.e. if we want to fit to the data just by decoupling the contributions from new physics, the mass of the Higgs boson is bounded as [16]

$$M_{\text{Higgs}} \lesssim 250 \text{ GeV}. \quad (4)$$

We then find from Eq. (1) that the values of $|m_h^2|$, and thus $|\delta m_h^2|$, should not be much larger than about $(310 \sim 400 \text{ GeV})^2$. This still places strong constraints on the sizes of $m_{\tilde{t}}^2$ and $\ln(M_{\text{mess}}/m_{\tilde{t}})$. We find that *even with an additional contribution to M_{Higgs} other than that in the MSSM, M_{mess} should still be much smaller than the Planck scale and $m_{\tilde{t}}^2$ is still subject to upperbounds that depend on the values of M_{mess}* . This is the key observation leading to the framework discussed in the next section.

3 Dynamical Breaking of Supersymmetry and $SU(5)$

We here specify our framework more explicitly. Because of small values of M_{mess} , we assume that supersymmetry breaking in the DSB sector is transmitted to the supersymmetric standard model sector through 321 gauge interactions. The gaugino and sfermion masses are then generated by the diagrams in Fig. 1. (The diagram giving the gaugino masses may be different; see discussion in section 6.) Here, the gray disks at the centers represent the contributions from the DSB sector, or some sector that feels primary supersymmetry breaking such as the messenger sector in gauge mediation models [10, 17]. We call this sector, collectively, the supersymmetry breaking sector.

There is an immediate consequence of mediating supersymmetry breaking by 321 gauge interactions. Suppose that the supersymmetry breaking sector carries the Dynkin index \hat{b} under

⁶Note that Eq. (1) applies not only to the MSSM but also to more general supersymmetric extensions of the standard model. Our argument is also independent of the origin of the supersymmetric Higgs mass μ . For example, μ may arise from the expectation value of a singlet field at the weak scale.

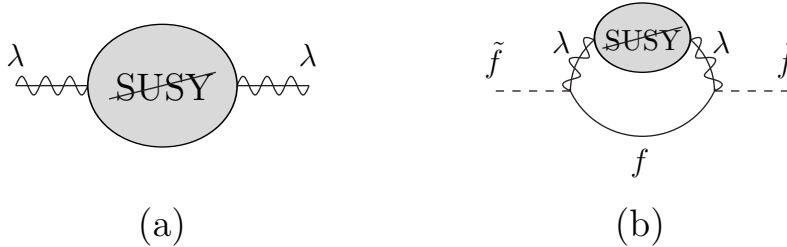


Figure 1: Examples of the diagrams that give (a) gaugino masses and (b) sfermion masses, where λ , \tilde{f} and f represent gauginos, sfermions and fermions, respectively.

$SU(3)_C$, $SU(2)_L$ and $U(1)_Y$, so that it contributes to the beta-function coefficients for the 321 gauge couplings by \hat{b} (the quantity \hat{b} should be universal for $SU(3)_C$, $SU(2)_L$ and $U(1)_Y$ in order not to destroy gauge coupling unification). The requirement that the 321 gauge couplings do not hit the Landau pole below the unification scale then gives a constraint $\hat{b} \lesssim 5$, where we have taken $M_{\text{mess}} = O(10 \sim 100 \text{ TeV})$. Now, the masses of the gauginos \tilde{M} and the sfermions \tilde{m} are generated at M_{mess} as threshold effects, through the diagrams in Fig. 1. Therefore, their values are bounded as $\tilde{M} \lesssim (g^2/16\pi^2)\hat{b}M_{\text{mess}}$ and $\tilde{m}^2 \lesssim (g^2/16\pi^2)^2 C \hat{b} M_{\text{mess}}^2$, where g and C represent the standard model gauge coupling and a Casimir factor. This gives a lower bound on the mediation scale $M_{\text{mess}} \gtrsim 20 \text{ TeV}$, and thus the size of the logarithm $\ln(M_{\text{mess}}/m_{\tilde{t}}) \gtrsim 3.5$. Using Eq. (2), we then find a rough upperbound on $m_{\tilde{t}}$ (and on generic squark masses $m_{\tilde{q}}$):

$$m_{\tilde{q}} \sim m_{\tilde{t}} \lesssim (660 \sim 850) \left(\frac{M_{\text{Higgs}}}{250 \text{ GeV}} \right) \text{ GeV}, \quad (5)$$

where the first relation comes from flavor universality. (In a realistic theory the lightest top-squark mass is somewhat smaller than the other squark masses by the top-Yukawa and left-right mixing effects.) Here, we have explicitly shown the dependence of the bound on the physical Higgs-boson mass, M_{Higgs} , coming from Eq. (1), to make it clear that the bound becomes tighter for smaller values of M_{Higgs} .

The naturalness bound derived above gives an immediate tension with the unified mass relation of Eq. (3), with the LEP II bound of $m_{\tilde{e}} \gtrsim 100 \text{ GeV}$. We find that the unified mass relation is not compatible with the naturalness bound unless the mass of the physical Higgs boson is rather large, $M_{\text{Higgs}} \gtrsim 200 \text{ GeV}$, which is consistent with the precision electroweak data only if the top-quark mass lies in the upper edge of the latest world average $m_t = 178.0 \pm 4.3 \text{ GeV}$ [18]. For $M_{\text{Higgs}} \gtrsim 200 \text{ GeV}$, having the right-handed selectron mass as small as its experimental lower bound, $m_{\tilde{e}} \simeq 100 \text{ GeV}$, allows the required amount of cancellations to be reduced to the level of 30% even with the unified mass relation of Eq. (3). Predictions of such a scenario, then, would

be a heavy Higgs boson, $M_{\text{Higgs}} \simeq (200 \sim 250)$ GeV, a heavy top quark, $m_t \simeq (180 \sim 182)$ GeV, light right-handed sleptons, $m_{\tilde{e}} \simeq 100$ GeV, and sfermions with masses given by the unified mass relations: $m_{\tilde{q}} \simeq m_{\tilde{u}} \simeq m_{\tilde{d}} \simeq 750$ GeV and $m_{\tilde{l}} \simeq 200$ GeV. However, the viability of this scenario depends crucially on the mass of the top quark. For example, if the top-quark mass is within the 1σ region of the recently reported CDF Run II value $m_t = 173.5 \pm 4.1$ GeV [19], the possibility of having the unified mass relation without fine-tuning disappears. We thus conclude that *unless the top-quark mass is in the upper edge of the experimentally allowed range, the unified mass relation of Eq. (3) is not compatible with the requirement from naturalness*. In the rest of the paper, we only consider the case in which the unified mass relation is violated.

We can also obtain a naturalness upperbound on the masses of the sleptons in a similar way. Mediations of supersymmetry breaking by 321 gauge interactions imply that the masses of the doublet sleptons are the same as m_h^2 before taking into account the effects from the Yukawa couplings. This implies that these masses should not be much larger than m_h^2 , giving

$$m_{\tilde{l}} \lesssim (310 \sim 400) \left(\frac{M_{\text{Higgs}}}{250 \text{ GeV}} \right) \text{ GeV}. \quad (6)$$

The bound on the singlet slepton masses is more indirect, but we expect that it is not much different from Eq. (6). This is because the difference of the doublet and singlet slepton masses arises only from the $SU(2)_L$ contribution and the factor 2 difference of hypercharges. These effects are not much larger than the values in Eq. (6) themselves and also work in opposite directions. It is important here to notice that the bounds in Eqs. (5, 6) rely only on $M_{\text{mess}} \gtrsim 20$ TeV. *They do not depend on any details of the supersymmetry breaking mechanism or on the origin of the additional contribution to the physical Higgs-boson mass.*

Now, let us consider properties of the supersymmetry breaking sector. The basic requirements on this sector are (i) it contributes to the evolution of the 321 gauge couplings universally, but (ii) it generates superparticle masses at M_{mess} that do not obey simple $SU(5)$ relations such as the one given in Eq. (3). It is, of course, possible that these requirements are satisfied simply because the matter content of the supersymmetry breaking sector fills out complete $SU(5)$ multiplets but the couplings in this sector do not respect $SU(5)$ at all.⁷ In this case, however, we should regard the appearance of the complete $SU(5)$ multiplets somewhat accidental.⁸ Moreover, if the supersymmetry breaking sector is strongly coupled over a wide energy interval above the weak scale, we expect non-universal corrections to the evolution of the 321 gauge couplings at higher loops, which are not necessarily suppressed. Therefore, here we consider an alternative

⁷An example of such theories is given by models of gauge mediation with non-minimal messenger sectors [4, 20].

⁸A class of “natural” models, however, arises if the messenger fields of gauge mediation live in the bulk of higher dimensional unified theories realized at the scale of $1/R \simeq (10^{15} \sim 10^{16})$ GeV, since these fields then have the 321 quantum numbers coming from an $SU(5)$ multiplet but do not obey any $SU(5)$ relations [21].

possibility that the supersymmetry breaking sector in fact possesses a global $SU(5)$ symmetry, of which the $SU(3) \times SU(2) \times U(1)$ subgroup is explicitly gauged and identified as the standard model gauge group. In this case the global $SU(5)$ symmetry ensures that the contribution to the 321 gauge coupling evolution from the supersymmetry breaking sector is universal. On the other hand, the effect of this $SU(5)$ symmetry should be absent in the spectrum of superparticles, as otherwise it would lead to the unified mass relations such as the one in Eq. (3). How can this happen?

The simplest possibility to realize the situation described above is to consider that the DSB sector possesses a global $SU(5)$ symmetry, of which the 321 subgroup is gauged and identified as the standard model gauge group, and to assume that the dynamics of this sector breaks not only supersymmetry but also the global $SU(5)$ symmetry to the 321 subgroup at the dynamical scale $\Lambda \approx M_{\text{mess}} \simeq (10 \sim 100)$ TeV. In this case the gray disks in Fig. 1 represent the DSB sector itself, and not some other sector feeling the primary supersymmetry breaking more directly than the supersymmetric standard model sector. This setup also has an advantage that the lowest possible values of M_{mess} are obtained, as the mediation of supersymmetry breaking is most direct. Because of the spontaneous breakdown of $SU(5)$ at the scale Λ , where the superparticle masses are generated, the resulting superparticle spectrum does not respect unified mass relations. A class of theories implementing this mechanism was first constructed in Ref. [3] in holographic higher dimensional spacetime, and was used in [4] to ameliorate fine-tuning in the context of specific models. Here, we will work in a more general context: we allow an arbitrary form of the Higgs potential and/or an arbitrary origin for the additional contribution to M_{Higgs} . The main conclusions of our analysis also do not depend on the mechanism of gaugino mass generation, as will be discussed in detail in section 6.

4 TeV-Scale Exotic Scalars

The framework described in the previous section has one general consequence. Because of the spontaneous breakdown of the global $SU(5)$ group to the 321 subgroup, the spectrum in the DSB sector contains light scalar particles, whose 321 gauge quantum numbers are the same as the unified gauge bosons (XY gauge bosons): $(\mathbf{3}, \mathbf{2})_{-5/6}$. The original global $SU(5)$ symmetry is also explicitly broken by the gauging of the 321 subgroup. Therefore, these particles are pseudo-Goldstone bosons and obtain masses at loop level through 321 gauge interactions. Since both $SU(5)$ and supersymmetry are broken at the scale $\Lambda \approx M_{\text{mess}}$, their masses squared are generically of order $(g^2 C / 16\pi^2) M_{\text{mess}}^2$. We call these light scalar particles *xyons*. Note that the superpartners of xyons obtain masses of order M_{mess} because of the supersymmetry breaking at the scale Λ .

It is possible that the DSB sector has a global symmetry larger than $SU(5)$, in which case the 321 quantum numbers of xyons are more complicated. For example, if the global group of the DSB sector is $SO(10)$ and spontaneously broken to the $SU(4)_C \times SU(2)_L \times SU(2)_R$ subgroup at the scale Λ , as is the case considered in Ref. [22], the 321 quantum numbers of xyons are given by $(\mathbf{3}, \mathbf{2})_{-5/6} + (\mathbf{3}, \mathbf{2})_{1/6}$.

4.1 Xyon mass — estimate

We here estimate the mass of xyons using naive scaling arguments. Since the xyon mass is generated at one loop through 321 gauge interactions, the mass squared m_φ^2 for xyons is roughly given by

$$m_\varphi^2 \simeq \sum_{i=1,2,3} \frac{g_i^2 C_i^\varphi}{16\pi^2} M_\rho^2, \quad (7)$$

where g_i are the 321 gauge couplings with $i = 1, 2, 3$ representing $U(1)_Y$, $SU(2)_L$ and $SU(3)_C$, and C_i^φ are the group theoretical factors: $(C_1^\varphi, C_2^\varphi, C_3^\varphi) = (5/12, 3/4, 4/3)$ for $SU(5)$ xyons. The parameter M_ρ is defined to be the mass scale for the resonances in the DSB sector ($M_\rho \approx \Lambda \approx M_{\text{mess}}$). The xyon mass is essentially determined by the quantity M_ρ .

Since the DSB sector generates the superparticle masses through 321 gauge interactions, the size of M_ρ is related to these masses. The gaugino masses are generated by the diagram in Fig. 1a, and given by

$$M_i \simeq g_i^2 \frac{\hat{b}}{16\pi^2} (\hat{\zeta}_i M_\rho), \quad (8)$$

where $\hat{\zeta}_i$ are parameters of $O(1)$ which can take different values for $i = 1, 2, 3$ reflecting the spontaneous breakdown of the global $SU(5)$ symmetry. This expression can be obtained using large- N scaling, by identifying the effective number of “colors” in the DSB sector as \hat{b} , the contribution of the DSB sector to the evolution of the 321 gauge couplings, which is appropriate in the present context. The scalar masses are similarly given by

$$m_{\tilde{f}}^2 \simeq 2 \sum_{i=1,2,3} \frac{g_i^4 C_i^{\tilde{f}}}{16\pi^2} \frac{\hat{b}}{16\pi^2} (\hat{\zeta}_i M_\rho)^2, \quad (9)$$

where $\tilde{f} = \tilde{q}, \tilde{u}, \tilde{d}, \tilde{l}, \tilde{e}$ represents the MSSM squarks and sleptons, and $C_i^{\tilde{f}}$ are the group theoretical factors given by $(C_1^{\tilde{f}}, C_2^{\tilde{f}}, C_3^{\tilde{f}}) = (1/60, 3/4, 4/3), (4/15, 0, 4/3), (1/15, 0, 4/3), (3/20, 3/4, 0)$ and $(3/5, 0, 0)$ for $\tilde{f} = \tilde{q}, \tilde{u}, \tilde{d}, \tilde{l}$ and \tilde{e} , respectively (the equation also applies to the Higgs fields with $C_i^h = C_i^{\tilde{h}} = C_i^{\tilde{j}}$). Here, the overall factor of 2 has been inserted so that the expression smoothly matches to the general gauge mediation result.

The size of M_ρ is determined by the superparticle masses through Eqs. (8, 9). Let us now assume that the masses of the squarks are dominated by the $SU(3)_C$ contributions, which is a

natural assumption given the bound in Eq. (6). The gluino mass $M_{\tilde{g}} = M_3$ is given by

$$M_{\tilde{g}} \simeq \frac{g_3^2 \hat{b}}{16\pi^2} (\hat{\zeta}_3 M_\rho), \quad (10)$$

while the squark mass squared $m_{\tilde{q}}^2 \sim m_{\tilde{t}}^2$ is given by

$$m_{\tilde{q}}^2 \simeq \frac{g_3^4 \hat{b}}{96\pi^4} (\hat{\zeta}_3 M_\rho)^2. \quad (11)$$

We thus find that the “size” of the DSB gauge group \hat{b} is given by

$$\hat{b} \simeq \frac{8}{3} \frac{M_{\tilde{g}}^2}{m_{\tilde{q}}^2}. \quad (12)$$

Note that $M_{\tilde{g}}$ and $m_{\tilde{q}}$ are the renormalized masses at the scale $\approx M_{\text{mess}}$. The corresponding equation in terms of the pole masses contains an extra factor of $(g_3(M_{\text{mess}})/g_3(M_{\tilde{g}}))^4$ in the right-hand-side.

The xyon mass is also dominated by the $SU(3)_C$ contribution. From Eq. (7), we find

$$m_\varphi^2 \simeq \frac{g_3^2}{12\pi^2} M_\rho^2. \quad (13)$$

The equations (11, 13) then tell us

$$m_\varphi^2 \simeq \frac{8\pi^2}{g_3^2} \frac{1}{\hat{b} \hat{\zeta}_3^2} m_{\tilde{q}}^2 \simeq (4m_{\tilde{q}})^2 \left(\frac{5}{\hat{b}}\right) \left(\frac{1}{\hat{\zeta}_3}\right)^2, \quad (14)$$

where we have used $g_3 = g_3(M_{\text{mess}}) \simeq 1$. This implies that if the “size” of the DSB sector \hat{b} is close to its maximum value 5, which is in fact naturally the case in the holographic theories discussed in the next subsection, the xyon mass is in the multi-TeV region. For $\hat{b} \simeq 5$ and $\hat{\zeta}_3 \simeq 1$, Eqs. (5, 14) gives

$$m_\varphi \lesssim 3 \text{ TeV}, \quad (15)$$

which is encouraging for the search for xyons at the LHC.⁹

The value of $\hat{\zeta}_3$ may be somewhat suppressed to give squark masses smaller than their “unified theoretic” values, i.e. the values given by the unified mass relations as in Eq. (3). To get some

⁹It should be noted that the estimate given here is very rough. Since the mass of xyons is quadratically divergent in the low-energy effective theory below M_ρ , its precise value depends on the details of the DSB sector. In the low-energy theory, this uncertainty can manifest in the fact that the M_ρ 's appearing in Eq. (7) and in Eqs. (8, 9) are not generically equal. The numbers for the xyon mass in this subsection, therefore, should be regarded only as a rough guide. The xyon mass is calculated in the next subsection in an explicit ultraviolet theory.

feeling about this potential suppression, we can take the ratio between the squark mass given in Eq. (11) and the right-handed selectron mass given by Eq. (9), which leads to

$$\frac{\hat{\zeta}_3}{\hat{\zeta}_1} \simeq \sqrt{\frac{9}{20} \frac{g_1^2 m_{\tilde{q}}}{g_3^2 m_{\tilde{e}}}} \simeq 0.15 \frac{m_{\tilde{q}}}{m_{\tilde{e}}}. \quad (16)$$

We then find that for values of squark and slepton masses that satisfy the naturalness bounds of Eqs. (5, 6) and the experimental constraints, the ratio of the $\hat{\zeta}$ parameters is naturally in a range $0.2 \lesssim \hat{\zeta}_3/\hat{\zeta}_1 \lesssim 0.8$. If we rewrite Eq. (14) in terms of $m_{\tilde{e}}$, using Eq. (16), we obtain

$$m_\varphi^2 \simeq (27m_{\tilde{e}})^2 \left(\frac{5}{\tilde{b}}\right) \left(\frac{1}{\hat{\zeta}_1}\right)^2. \quad (17)$$

This implies that if the violation of the unified mass relations is entirely due to a suppression of squark masses by $\hat{\zeta}_3 < 1$, and not due to an enhancement of slepton masses by $\hat{\zeta}_1 > 1$, the mass of xyons is larger than about 3 TeV, in which case the discovery of xyons at the LHC may be difficult. It is, however, plausible that the violation of the unified mass relations is a combined effect of both $\hat{\zeta}_3 < 1$ and $\hat{\zeta}_1 > 1$. In this case it is possible that xyons will in fact be discovered at the LHC.

4.2 Holographic theories in warped space

We here consider a class of calculable theories that naturally realizes the framework discussed in section 3. Suppose that the size (the number of “colors”) \tilde{N} of the DSB gauge group is large: $\tilde{N} \gg 1$. In this case, the DSB sector produces a large number of hadronic resonances at the scale Λ , whose interaction strengths are suppressed by powers of $1/\sqrt{\tilde{N}}$ [23]. This suggests that the theory may have an equivalent but different description based on these weakly coupled resonances. In fact, the gauge/gravity duality suggests that under certain conditions these resonances are identified as the Kaluza-Klein (KK) towers in some higher dimensional theory and that we can formulate the theory in higher dimensional spacetime compactified to four dimensions.

To be more explicit, let us assume that the gauge coupling \tilde{g} of the DSB gauge interaction is nearly conformal above Λ , i.e. it evolves very slowly over a wide energy interval between Λ and a high scale of order the unification scale $M_X \simeq 10^{16}$ GeV, and that it takes a value $\tilde{g}^2 \tilde{N}/16\pi^2 \gg 1$. The AdS/CFT correspondence then suggests that we may formulate our theory in 5D anti-de Sitter (AdS) space truncated by two branes [24]. The metric of this spacetime is given by

$$ds^2 \equiv G_{MN} dx^M dx^N = e^{-2k|y|} \eta_{\mu\nu} dx^\mu dx^\nu + dy^2, \quad (18)$$

where y is the coordinate for the extra dimension and k denotes the inverse curvature radius of the AdS space. The two branes are located at $y = 0$ (the UV brane) and $y = \pi R$ (the IR brane). This is the spacetime considered in Ref. [25], in which the large hierarchy between the weak and the Planck scales is generated by the AdS warp factor. The scales are chosen such that the scales on the UV and IR branes are roughly the 4D Planck scale and the scale Λ , respectively: $k \sim M_5 \sim M_* \sim M_{\text{Pl}}$ and $kR \sim 10$ (the 4D Planck scale is given by $M_{\text{Pl}}^2 \simeq M_5^3/k$). Here, M_5 is the 5D Planck scale, and M_* the 5D cutoff scale, which is taken to be somewhat (typically a factor of a few) larger than k . With this choice of scales, the characteristic mass scale for the KK towers, which are 5D manifestations of the resonances in the DSB sector, is given by $\pi k e^{-\pi k R} \sim \Lambda \approx (10 \sim 100)$ TeV.

Strictly speaking, to have a “dual” higher dimensional description considered here, the “original” 4D theory must possess certain non-trivial properties such as the existence of mass gaps between the resonances with spins ≤ 2 and those with higher spins. However, once we have the picture of 5D warped space and construct a theory on this space, we can forget about the “original” 4D picture for all practical purposes and work out all physical consequences using higher dimensional effective field theories. This viewpoint was particularly emphasized in [26], which we follow here. Note that the xyon mass calculated below is dominated by the momentum region around Λ , so that the precise geometry in the ultraviolet region is not important — it can deviate from the pure AdS without changing the essential result.

Since the global symmetry of the DSB sector corresponds to the gauge symmetry in the 5D picture, the minimal theory in 5D warped space has a gauge group $SU(5)$ in the bulk. We thus consider a supersymmetric $SU(5)$ gauge theory on the truncated 5D warped spacetime, Eq. (18). The bulk $SU(5)$ symmetry is broken to the 321 subgroup at the UV brane, reflecting the fact that only the 321 subgroup is gauged in the 4D picture (at least at scales below M_X). At the IR brane, both $SU(5)$ and supersymmetry are broken, reflecting the fact that these symmetries are both broken by the dynamics of the DSB sector; specifically, the $SU(5)$ symmetry is also broken to the 321 subgroup on this brane. This class of theories was first constructed in Ref. [3], and we refer the readers there for further details. The locations of the matter and Higgs fields are somewhat model dependent; the only restriction is that, to preserve the successful supersymmetric prediction for gauge coupling unification, the wavefunctions for the zero modes of these fields are either localized to the UV brane or conformally flat [27] (for earlier work see [28]). Here we simply put three generations of the quark and lepton superfields Q, U, D, L and E (and the right-handed neutrinos N) on the UV brane, and locate the Higgs fields, $\mathbf{5} + \mathbf{5}^*$ of $SU(5)$, in the bulk. The case of bulk matter will be discussed in subsection 4.4. The Yukawa couplings are located on the UV brane. This setup leads to fully realistic phenomenologies — proton decay is sufficiently suppressed and small neutrino masses are naturally obtained through

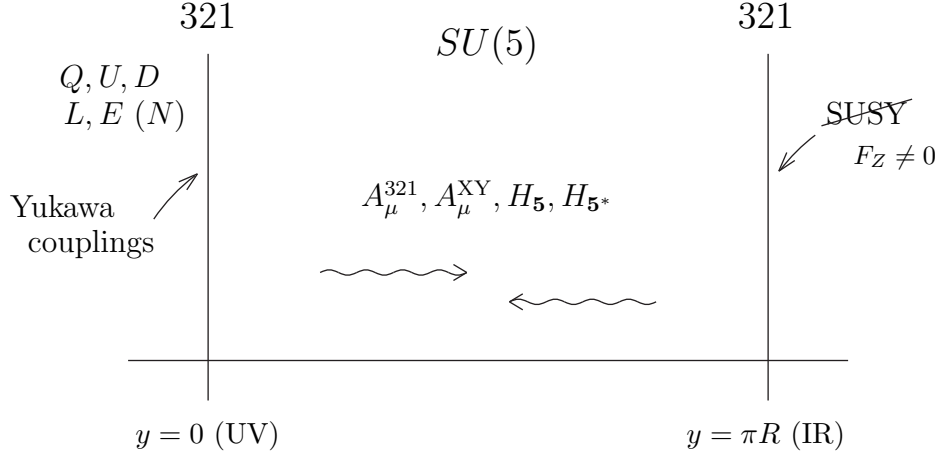


Figure 2: The overall picture of the theory.

the seesaw mechanism. The overall picture of the theory is depicted in Fig. 2.

How do xyons arise in this theory? According to the general discussion at the beginning of this section, the theory must produce relatively light scalar particles that have the same 321 gauge quantum numbers as the XY gauge bosons. To see this explicitly, we here adopt a simple mechanism of breaking $SU(5)$ by boundary conditions both at the UV and IR branes.¹⁰ The boundary conditions on the 5D gauge multiplet are given by

$$\begin{pmatrix} V \\ \Sigma \end{pmatrix} (x^\mu, -y) = \begin{pmatrix} \hat{P}V\hat{P}^{-1} \\ -\hat{P}\Sigma\hat{P}^{-1} \end{pmatrix} (x^\mu, y), \quad \begin{pmatrix} V \\ \Sigma \end{pmatrix} (x^\mu, -y') = \begin{pmatrix} \hat{P}V\hat{P}^{-1} \\ -\hat{P}\Sigma\hat{P}^{-1} \end{pmatrix} (x^\mu, y'), \quad (19)$$

where $y' = y - \pi R$, and \hat{P} is a 5×5 matrix acting on gauge space: $\hat{P} = \text{diag}(+, +, +, -, -)$. Here, we have represented the 5D gauge multiplet in terms of a 4D $N = 1$ vector superfield $V(A_\mu, \lambda)$ and a 4D $N = 1$ chiral superfield $\Sigma(\chi + iA_5, \lambda')$, both of which are in the adjoint representation of $SU(5)$, and given the above boundary conditions in the orbifold picture. The boundary conditions for the Higgs multiplets are given similarly. Using notation where a bulk hypermultiplet is represented by two 4D $N = 1$ chiral superfields $\Phi(\phi, \psi)$ and $\Phi^c(\phi^c, \psi^c)$ with opposite quantum numbers, the two Higgs hypermultiplets $\{H, H^c\}$ and $\{\bar{H}, \bar{H}^c\}$ obey boundary conditions similar to Eq. (19), i.e. \hat{P} acting on the $SU(5)$ fundamental indices, with V and Σ replaced by H and H^c (\bar{H} and \bar{H}^c), respectively.¹¹

¹⁰The $SU(5)$ breaking on the UV and/or IR branes can be due to vacuum expectation values (VEVs) of $SU(5)$ -breaking Higgs fields located on the UV and/or IR branes. This does not change any of the essential physics discussed here, as long as the VEV on the IR brane is sufficiently larger than the local AdS curvature scale and the VEV on the UV brane is of order k or larger. In the case that the UV-brane VEV is smaller, the estimate on the xyon mass could be affected. We will comment on this case at the end of subsection 4.3.

¹¹The boundary conditions for the Higgs multiplets on the IR brane can be reversed without destroying the

The spectrum of the model in the supersymmetric limit is then given as follows [3]. For the gauge sector, the KK spectrum of the gauge tower, m_n , is approximately given by

$$\left\{ \begin{array}{l} V^{321} : \quad m_0 = 0, \\ \{V^{321}, \Sigma^{321}\} : \quad m_n \simeq (n - \frac{1}{4})\pi k', \end{array} \right. \quad \left\{ \begin{array}{l} \Sigma^{XY} : \quad m_0 = 0, \\ \{V^{XY}, \Sigma^{XY}\} : \quad m_n \simeq (n + \frac{1}{4})\pi k', \end{array} \right. \quad (20)$$

where $n = 1, 2, \dots$, and $k' \equiv ke^{-\pi kR} \approx (10 \sim 100)$ TeV is the rescaled AdS curvature scale. An important point is that the zero modes consist of not only the 321 component of V , V^{321} , but also the $SU(5)/321$ (XY) component of Σ , Σ^{XY} (this exotic state, however, does not affect the gauge coupling prediction nor lead to rapid proton decay [3]). The spectrum for the Higgs sector is model dependent; it depends on the choice of boundary conditions, the shape of the zero-mode wavefunctions, and a potential supersymmetric mass term on the IR brane.

After supersymmetry breaking, some of the zero-mode states obtain masses. Supersymmetry breaking is generically parameterized by an F -term vacuum expectation value (VEV) of a singlet chiral superfield Z localized on the IR brane [29, 27]. The 321 gauginos, λ^{321} , then obtain masses through the following operators on the IR brane:

$$S_{321} = \int d^4x \int_0^{\pi R} dy 2\delta(y - \pi R) \sum_{i=1,2,3} \left[- \int d^2\theta \frac{\zeta_i}{M_*} Z \text{Tr}[\mathcal{W}_i^\alpha \mathcal{W}_{i\alpha}] + \text{h.c.} \right], \quad (21)$$

where $\mathcal{W}_{i\alpha} \equiv -(1/8)\bar{D}^2(e^{-2V_i}\mathcal{D}_\alpha e^{2V_i})$ represent field-strength superfields, and $i = 1, 2, 3$ denotes $U(1)_Y$, $SU(2)_L$ and $SU(3)_C$, respectively. Note that the three coefficients ζ_i are in general not equal, reflecting the $SU(5)$ breaking on the IR brane, so that the 321 gaugino masses do not obey any unified relations in general. This is the 5D manifestation of the spontaneous $SU(5)$ breaking in the DSB sector.

Supersymmetry breaking also gives masses to zero modes in Σ^{XY} through the following operators on the IR brane:

$$S_{XY} = \int d^4x \int_0^{\pi R} dy 2\delta(y - \pi R) \left[\left\{ e^{-2\pi kR} \int d^4\theta \frac{\eta}{2M_*} Z^\dagger \text{Tr}[\mathcal{P}[\mathcal{A}]\mathcal{P}[\mathcal{A}]] + \text{h.c.} \right\} - e^{-2\pi kR} \int d^4\theta \frac{\rho}{4M_*^2} Z^\dagger Z \text{Tr}[\mathcal{P}[\mathcal{A}]\mathcal{P}[\mathcal{A}]] \right], \quad (22)$$

where $\mathcal{A} \equiv e^{-2V}(\partial_y e^{2V}) - \sqrt{2}e^{-2V}\Sigma^\dagger e^{2V} - \sqrt{2}\Sigma$.¹² Here, the trace is over the $SU(5)$ space and $\mathcal{P}[\mathcal{X}]$ is a projection operator: with \mathcal{X} an adjoint of $SU(5)$, $\mathcal{P}[\mathcal{X}]$ extracts the $(\mathbf{3}, \mathbf{2})_{-5/6} + (\mathbf{3}^*, \mathbf{2})_{5/6}$ component of \mathcal{X} under the decomposition to 321. The coefficients η and ρ are dimensionless parameters. Apparent singularities arising from taking the thin-wall limit for the IR

successes of the model.

¹²The expression for \mathcal{A} in Ref. [3] is valid only in the Wess-Zumino gauge. The expression here applies in arbitrary gauges [30].

brane are absorbed by appropriately redefining the coefficients of IR-brane operators. At the leading order

$$\rho = -8g_5^2|\eta|^2\delta(0) + \rho', \quad (23)$$

where g_5 is the 5D gauge coupling [3]. In the fundamental theory, these singularities are smoothed out by the effects of brane thickness, of order M_*^{-1} .

The operators in Eq. (22) give masses of order $\pi k'$ to the zero modes of λ^{XY} and χ^{XY} at tree level, but not to A_5^{XY} . In fact, we find that 5D gauge invariance forbids any local operator giving a mass to A_5^{XY} . The mass of A_5^{XY} is then generated only at loop level, and so is significantly smaller than those of the other XY states such as λ^{XY} and χ^{XY} . We thus find that the light states implied by the general argument are the zero modes of A_5^{XY} — *xyons in our theory arise from the extra dimensional component of the grand unified gauge bosons.*¹³

4.3 Superparticle and xyon masses

We are now ready to calculate the mass of xyons φ , or the zero modes of A_5^{XY} , as well as those of the MSSM superparticles, in the 5D theory. These masses depend on the unknown coefficients ζ_i , η and ρ' in Eqs. (21, 22, 23) and the F -term VEV of Z through the following combinations:

$$M_{\lambda,i} \equiv \frac{\zeta_i F_Z}{M_*}, \quad M_{\lambda,X} \equiv \frac{\eta F_Z^*}{M_*}, \quad M_{\chi,X}^2 \equiv \frac{\rho' |F_Z|^2}{M_*^2}, \quad (24)$$

where $i = 1, 2, 3$ and F_Z is the F -term VEV of Z defined by $\langle Z \rangle = -e^{-\pi k R} F_Z \theta^2$. The natural sizes for these parameters are estimated using naive dimensional analysis as $\zeta_i \sim 1/4\pi$, $\eta \sim 1/4\pi$, $\rho' \sim 1$ and $F_Z \sim M_*^2/4\pi$ [31]. We thus define dimensionless parameters

$$r_{\lambda,i} \equiv \frac{M_{\lambda,i}}{M_*/16\pi^2}, \quad r_{\lambda,X} \equiv \frac{M_{\lambda,X}}{M_*/16\pi^2}, \quad r_{\chi,X} \equiv \frac{M_{\chi,X}^2}{M_*^2/16\pi^2}, \quad (25)$$

which are all expected to be $O(1)$: $r_{\lambda,i} \sim r_{\lambda,X} \sim r_{\chi,X} \sim 1$. The masses of xyons and superparticles depend on these parameters as well as other model parameters, specifically $M_*/\pi k$ and $k' = k e^{-\pi k R}$.

The calculation of the masses is performed following the procedure of Ref. [32]. We first obtain the 5D action with all the couplings renormalized at a scale k' measured in terms of the 4D metric $\eta_{\mu\nu}$. The relevant ones are the bulk and brane gauge couplings, g_5 , $\tilde{g}_{0,i}$ and $\tilde{g}_{\pi,i}$:

$$S = -\frac{1}{4} \int d^4x \int_0^{\pi R} dy \sqrt{-G} \left[\frac{1}{g_5^2} F_{MN} F^{MN} + 2\delta(y) \frac{1}{\tilde{g}_{0,i}^2} F^i{}_{\mu\nu} F^{i\mu\nu} + 2\delta(y - \pi R) \frac{1}{\tilde{g}_{\pi,i}^2} F^i{}_{\mu\nu} F^{i\mu\nu} \right]. \quad (26)$$

¹³In general, if the $SU(5)$ breaking on the IR brane is caused by the VEV of a Higgs field localized on the IR brane, xyons are mixtures of the XY component of the brane Higgs field and the extra dimensional component of the grand unified gauge bosons.

Assuming that the sizes of these couplings are determined by naive dimensional analysis at the appropriate cutoff scale (see e.g. [27]), the values of the UV-brane couplings evaluated at k' are given by

$$\frac{1}{\tilde{g}_{0,i}^2} \simeq \frac{b_i^{\text{MSSM}}}{8\pi^2} \ln\left(\frac{k}{k'}\right), \quad (27)$$

where $(b_1^{\text{MSSM}}, b_2^{\text{MSSM}}, b_3^{\text{MSSM}}) = (33/5, 1, -3)$ are the MSSM beta-function coefficients, and k should be identified as the unification scale: $k \approx M_X \simeq 10^{16}$ GeV. The values of the IR-brane couplings are determined by naive dimensional analysis as $1/\tilde{g}_{\pi,i}^2 \sim C_i/16\pi^2$, where C_i are group theoretical factors of order one. Because there is no logarithmic enhancement for the IR-brane terms, we can safely neglect these terms and set $1/\tilde{g}_{\pi,i}^2 = 0$ in our calculation. (Neglecting the IR-brane terms yields errors of order $\pi k/M_* \simeq (20 \sim 50)\%$ for the xyon and sfermion squared-masses, but errors of this order are not very important for our discussion here.) Setting $1/\tilde{g}_{\pi,i}^2 = 0$, the 4D gauge couplings g_i at the scale k' are given by

$$\frac{1}{g_i^2} = \frac{\pi R}{g_5^2} + \frac{1}{\tilde{g}_{0,i}^2}. \quad (28)$$

This determines the bulk gauge coupling, g_5 , in terms of the 4D gauge couplings, g_i , and the UV-brane couplings evaluated at the scale k' , given by Eq. (27).

The masses of the gauginos and sfermions are calculated as in [32], but now the gaugino mass parameters at the IR brane for $SU(3)_C$, $SU(2)_L$ and $U(1)_Y$ are not necessarily equal: $M_{\lambda,1} \neq M_{\lambda,2} \neq M_{\lambda,3}$. The results of the calculation are summarized in Appendix A. In Fig. 3 we illustrate the behavior of the gaugino and sfermion masses as functions of $r_{\lambda,i}$ for $k' = 10$ TeV and $M_*/\pi k' = 3$. Here, the masses are the running masses but evolved down to the scale of superparticle masses, so that they are close to the pole masses. The solid lines represent the gaugino masses for $SU(3)_C$, $SU(2)_L$ and $U(1)_Y$ from above, and the horizontal axis represents $r_{\lambda,3}$, $r_{\lambda,2}$, and $r_{\lambda,1}$, respectively, for each gaugino-mass line. The dashed lines represent the sfermion masses ($m_{\tilde{q}}$, $m_{\tilde{u}}$, $m_{\tilde{d}}$, $m_{\tilde{l}}$ and $m_{\tilde{e}}$ from above) with $m_{\tilde{q}}$, $m_{\tilde{u}}$, and $m_{\tilde{d}}$ closely spaced and $m_{\tilde{l}}$ and $m_{\tilde{e}}$ below. To draw the sfermion-mass lines, we have taken $r_{\lambda,1} = r_{\lambda,2} = r_{\lambda,3}$ for simplicity; however, we can use Fig. 3 in the general case of $r_{\lambda,1} \neq r_{\lambda,2} \neq r_{\lambda,3}$ to obtain approximate values for the sfermion masses by identifying the horizontal axis to be $r_{\lambda,3}$ for $\{m_{\tilde{q}}, m_{\tilde{u}}, m_{\tilde{d}}\}$, $r_{\lambda,2}$ for $m_{\tilde{l}}$, and $r_{\lambda,1}$ for $m_{\tilde{e}}$. For different values of k' the masses scale linearly in k' . Taking different values of $M_*/\pi k'$ results in rescaling the horizontal axis, as the effects of $M_*/\pi k' \rightarrow \alpha(M_*/\pi k')$ is the same as those of $r_{\lambda,i} \rightarrow \alpha r_{\lambda,i}$ with a fixed value of k' .

It may be useful here to present the approximate formulae for the gaugino and sfermion masses, derived in [26]. These formulae are obtained by working out the correspondence relations

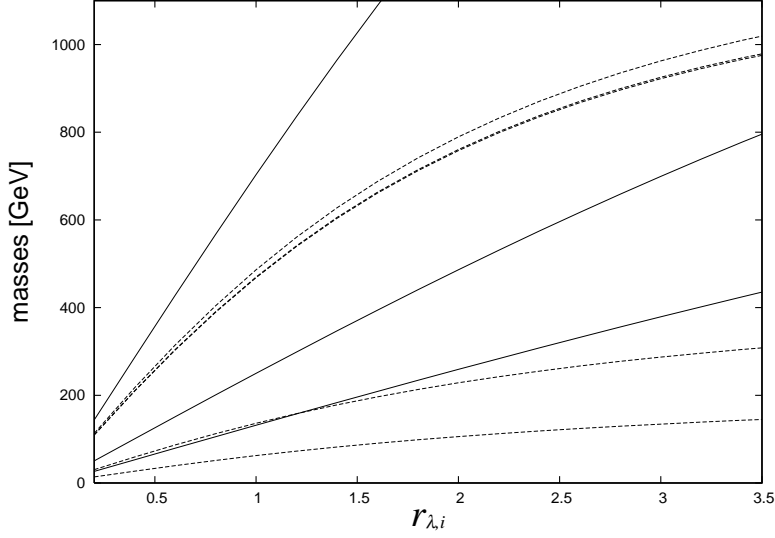


Figure 3: Masses of the MSSM gauginos (solid, with M_3 , M_2 and M_1 from above) and the MSSM scalars (dashed, with $m_{\tilde{q}}$, $m_{\tilde{u}}$, and $m_{\tilde{d}}$ closely spaced and $m_{\tilde{l}}$ and $m_{\tilde{e}}$ below). The horizontal axis represents dimensionless parameters $r_{\lambda,i}$ as explained in the text.

between the 4D and 5D theories, which are given by

$$M_\rho \approx \pi k', \quad \frac{\hat{b}}{8\pi^2} \approx \frac{1}{g_5^2 k}, \quad \hat{\zeta}_i \approx \frac{2g_5^2 F_Z}{\pi M_*} \zeta_i. \quad (29)$$

Using these relations in Eqs. (8, 9), we obtain the formulae for the gaugino masses

$$M_i \simeq g_i^2 M'_{\lambda,i}, \quad (30)$$

and the sfermion masses

$$m_{\tilde{f}}^2 \simeq \sum_{i=1,2,3} \frac{g_i^4 C_i^{\tilde{f}}}{4\pi^2} (g_5^2 k) M_{\lambda,i}^2, \quad (31)$$

where $M'_{\lambda,i} \equiv M_{\lambda,i} e^{-\pi k R} = (\zeta_i F_Z / M_*) (k' / k)$. The equations (30, 31) will reproduce the numerical results for the superparticle masses in the parameter region $\hat{\zeta}_i \simeq g_5^2 F_Z \zeta_i / M_* \lesssim O(1)$.

The parameter region leading to the desired pattern for the superparticle masses can be read off from Fig. 3, or Eqs. (30, 31). For example, we find that the desired pattern is obtained by taking

$$\{r_{\lambda,1}, r_{\lambda,2}, r_{\lambda,3}\} = \{2.5, 0.9, 1.0\}, \quad M_*/\pi k = 3, \quad k' = 10 \text{ TeV}, \quad (32)$$

which gives the soft supersymmetry breaking masses

$$M_1 \approx 320 \text{ GeV}, \quad M_2 \approx 230 \text{ GeV}, \quad M_3 \approx 700 \text{ GeV}, \quad (33)$$

for the gauginos and

$$m_{\tilde{g}}^2 \approx (480 \text{ GeV})^2, \quad m_{\tilde{u}}^2 \approx (470 \text{ GeV})^2, \quad m_{\tilde{d}}^2 \approx (470 \text{ GeV})^2, \quad (34)$$

$$m_{\tilde{t}}^2 \approx (140 \text{ GeV})^2, \quad m_{\tilde{e}}^2 \approx (120 \text{ GeV})^2, \quad (35)$$

for the squarks and sleptons.

The spectrum in Eqs. (33 – 35) has the following characteristic features.

- (A) Taking into account small mass splittings among the generations arising from the Yukawa couplings, the lightest among the MSSM gauginos, squarks and sleptons is the stau $\tilde{\tau}$, which is most likely the next-to-lightest supersymmetric particle (NLSP). (The lightest supersymmetric particle (LSP) is the gravitino, whose mass is of order $m_{3/2} \approx \Lambda^2/M_{\text{Pl}} \simeq (0.1 \sim 10) \text{ eV}$ unless there is some other source of supersymmetry breaking than the DSB sector considered.)
- (B) The 5D theory with small tree-level UV-brane gauge kinetic terms corresponds in 4D to a theory in which the standard model gauge couplings are large at the unification scale $M_X \simeq 10^{16} \text{ GeV}$ (see Ref. [27]). This implies $\hat{b} \simeq 5$, and we find from Eqs. (8, 9), or Eqs. (30, 31), that $M_3/m_{\tilde{q},\tilde{u},\tilde{d}} \approx (3\hat{b}/8)^{1/2} \simeq 1.4$ and $M_2/m_{\tilde{t}} \approx (2\hat{b}/3)^{1/2} \simeq 1.8$. (The corresponding relation for $U(1)_Y$, $M_1/m_{\tilde{e}} \approx (5\hat{b}/6)^{1/2} \simeq 2.0$, does not hold well because the value of ζ_1 , or $\hat{\zeta}_1$, $r_{\lambda,i}$, is outside the region where the approximate mass formulae apply.)
- (C) The masses of the squarks are close with each other. They are larger than the slepton masses but only by a factor of a few. In particular, the ratio of the squark to the slepton masses is smaller than that given by the unified mass relations.
- (D) The Higgsino mass parameter μ inferred from Eq. (1) is generically small, $|\mu| \lesssim 200 \text{ GeV}$ for $\tan \beta \gtrsim 2$, if we require the amount of fine-tuning to be smaller than 20%. Therefore, if the Higgs sector has a certain resemblance to that of the MSSM, the two lightest neutralinos and the lighter chargino tend to have closer masses. The value of $|\mu|$, however, can be larger if $\tan \beta$ is smaller, due to a larger value of y_t . (Note that $\tan \beta$ as small as $\simeq 1.2$ is possible in the present theory because the evolution of the top Yukawa coupling is strongly asymptotically free due to larger values of the $SU(3)_C$ gauge coupling at high energies.) In general, μ is bounded as $|\mu| \lesssim (310 \sim 400) \text{ GeV}$ (see Eq. (1) and the discussion below Eq. (4)), so that there are at least two neutralinos and a chargino with masses below $\simeq 400 \text{ GeV}$.

In fact, these features are somewhat generic in our scenario because they arise mainly from the gauge mediated nature of supersymmetry breaking and the relations between the gaugino mass parameters $r_{\lambda,2}, r_{\lambda,3} \lesssim r_{\lambda,1}$, which comes from the requirement of reducing the fine-tuning and

evading the experimental constraint $m_{\tilde{e}} \gtrsim 100$ GeV. It is, however, important to notice that they are also subject to some model dependencies. For instance, the mass ratios of gauginos to squarks and sleptons given in (B) become smaller if \tilde{b} is smaller, which can be the case if the $SU(5)$ breaking on the UV brane is due to the Higgs mechanism. The ratios may even be completely different if the mechanism of gaugino mass generation is different (see discussion in section 6). Also, the feature of (D) could depend on the detailed structure of the Higgs sector, which we do not specify explicitly in the present work. In fact, the structure of the Higgs sector in our scenario is expected to be (much) richer than that of the MSSM.

Here we note that the particular parameter point above has been chosen for illustrative purposes. Experimental constraints will realistically reduce the parameter space of our scenario, especially that coming from the $b \rightarrow s\gamma$ process. Determining the precise constraints on our parameter space is a complicated problem, mostly because of the theoretical uncertainties involved, and so we do not pursue it here. However, there is a large parametric freedom in our framework. For example, if it turns out that the above parameter point is problematic, we can increase the value of k' somewhat and/or change the ratios between $r_{\lambda,i}$'s, still keeping the fine-tuning small. Some of the constraints may also depend on the structure of the Higgs sector, which we have not specified in detail. The constraints are also different if the gauginos are Dirac fermions as in the model discussed in section 6.

We now turn to the xyon mass. The mass of xyons is obtained by calculating 5D one-loop diagrams. The details of the calculation are given in Appendix A. The xyon mass squared, m_{φ}^2 , is given in terms of the parameters $r_{\lambda,i}$, $r_{\lambda,X}$, $r_{\chi,X}$, $M_*/\pi k$ and k' . In general, m_{φ}^2 depends on the complex phases of the IR-brane supersymmetry breaking parameters $M_{\lambda,i}$ and $M_{\lambda,X}$ (i.e. the phases of $r_{\lambda,i}$ and $r_{\lambda,X}$), but as is discussed in Appendix A the dependence of m_{φ}^2 on these phases is small. We thus take $r_{\lambda,i}$ and $r_{\lambda,X}$ to be real in the analysis here (the other parameters, $r_{\chi,X}$, $M_*/\pi k$ and k' , are always real). The analysis in Appendix A also tells us the following. (i) The squared mass for xyons, m_{φ}^2 , is positive for most of the parameter region, which is crucial for the model to be viable. (ii) In a natural parameter region $r_{\lambda,i} \sim r_{\lambda,X} \sim r_{\chi,X} \sim O(1)$ the value of m_{φ}^2 depends practically only on $r_{\lambda,X}$, $M_*/\pi k$ and k' . (iii) The effect of $M_*/\pi k \rightarrow \alpha(M_*/\pi k')$ on m_{φ}^2 is the same as that of $r_{\lambda,X} \rightarrow \alpha r_{\lambda,X}$ with a fixed value of k' . (iv) The xyon mass, $(m_{\varphi}^2)^{1/2}$, scales almost linearly with k' .

The features (ii), (iii) and (iv) described above allows us to represent m_{φ}^2 as a function only of $r_{\lambda,X}$ with fixed values of the other parameters, since the dependence on the other parameters is either very weak or trivially reproduced. In Fig. 4 we plot the mass of xyons, $(m_{\varphi}^2)^{1/2}$ as a function of $r_{\lambda,X}$ for $k' = 8, 10$ and 13 TeV with the fixed values of $\{r_{\lambda,1}, r_{\lambda,2}, r_{\lambda,3}\} = \{2.5, 0.9, 1.0\}$, $r_{\chi,X} = 1$ and $M_*/\pi k = 3$. As discussed before (see Eq. (32) and discussions around), these values give the superparticle masses desired for electroweak symmetry breaking. The figure then shows that for

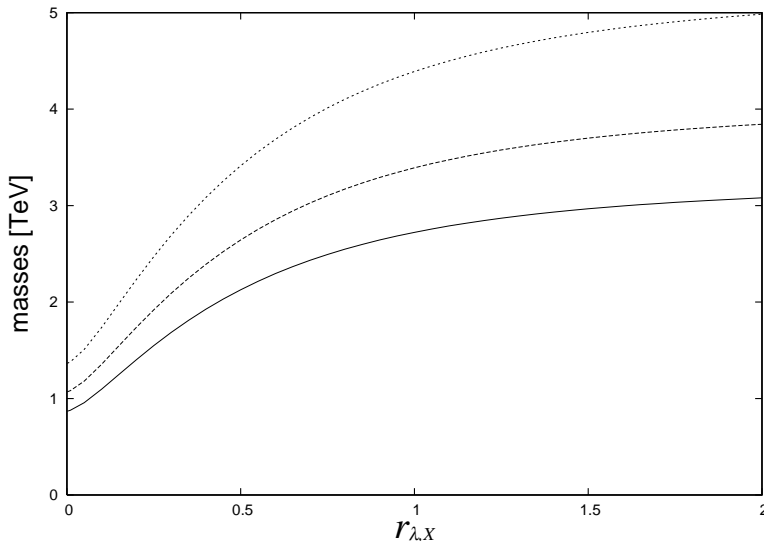


Figure 4: The mass of xyons as a function of $r_{\lambda, X}$ for $\{r_{\lambda,1}, r_{\lambda,2}, r_{\lambda,3}\} = \{2.5, 0.9, 1.0\}$, $r_{\chi, X} = 1$ and $M_*/\pi k = 3$. The three curves correspond to three different values of k' : $k' = 8$ TeV (solid) 10 TeV (dashed) and 13 TeV (dotted).

natural values of $r_{\lambda, X} \sim O(1)$, the mass of xyons lies in a range $1 \text{ TeV} \lesssim m_\varphi \lesssim 5 \text{ TeV}$. While the IR-brane operators neglected in our analysis can cause an error of order $\pi k/M_* \simeq 30\%$ in the xyon mass, we still conclude that *for natural values of the model parameters*, $r_{\lambda, i} \sim r_{\lambda, X} \sim r_{\chi, X} \sim O(1)$ and $M_*/\pi k$ a factor of a few, the mass of xyons is expected to lie in the multi-TeV region.¹⁴ This is encouraging for the discovery of xyons at the LHC. As we will discuss in subsection 5.1, the reach of the LHC in the xyon mass is about $(2.0 \sim 2.2) \text{ TeV}$. Therefore, for $k' = 8 \text{ TeV}$ (10 TeV), xyons may be discovered at the LHC if $r_{\lambda, i} \lesssim 0.6$ (0.4). It is also interesting that the mass of xyons saturates at larger values of $r_{\lambda, X}$. For example, the mass is bounded for $k' = 8, 10, 13 \text{ TeV}$ by $\approx 3, 4, 5 \text{ TeV}$, respectively. The discovery of xyons at the VLHC will, therefore, be quite promising.

A few comments are in order. We have calculated so far the mass of xyons in the theory where $SU(5)$ is broken by boundary conditions at the UV brane. This corresponds in the 4D picture to the case with $\hat{b} \simeq 5$, as the successful prediction for the low-energy gauge couplings requires the theory to be strongly coupled at the unification scale (the tree-level UV-brane gauge kinetic terms to be small). The breaking of $SU(5)$ on the UV brane, however, may also be due

¹⁴In the model of Ref. [4] where supersymmetry breaking is mediated to the Higgs sector through singlet fields, the scale of the IR brane tends to be higher, $k' = O(100 \text{ TeV})$, leading to $m_\varphi = O(10 \text{ TeV})$. This corresponds to the region where $r_{\lambda, i}$, or ζ_i , are smaller than the naive values, $r_{\lambda, i} = O(0.1)$. It is possible, however, to modify the Higgs sector to allow more direct mediation so that the naive values for the couplings are accommodated and that the xyon mass is lowered to the multi-TeV region.

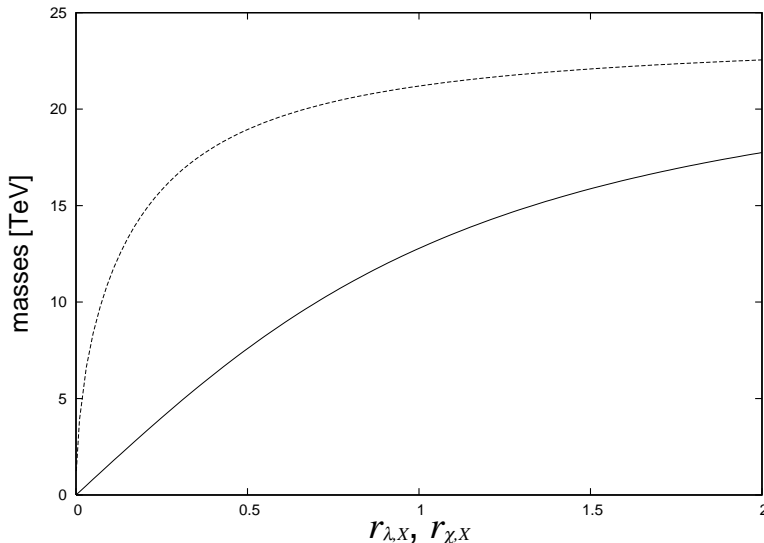


Figure 5: Masses of the superpartners of xyons, λ^{XY} (solid) and χ^{XY} (dashed), for $M_*/\pi k = 3$ and $k' = 10$ TeV. The horizontal axis represents $r_{\lambda,X}$ and $r_{\chi,X}$ for λ^{XY} and χ^{XY} , respectively.

to the Higgs mechanism. Then, if the VEV of the $SU(5)$ -breaking Higgs is sufficiently smaller than the cutoff scale M_* , we can have a sizable tree-level UV-brane gauge kinetic term without destroying the successful prediction. This corresponds in 4D to having small 321 gauge couplings at the unification scale and thus \hat{b} smaller than $\simeq 5$. This in turn raises the mass of xyons by a factor of $(5/\hat{b})^{1/2}$ compared with the values given in Fig. 4 (see e.g. Eqs. (14, 17)).

Finally, the masses of the superpartners of xyons are calculated using equations given in Appendix A. These masses are plotted in Fig. 5 for $M_*/\pi k = 3$ and $k' = 10$ TeV. Solid and dashed lines represent the fermionic and bosonic superpartners of xyons, λ^{XY} and χ^{XY} , respectively, and the horizontal axis corresponds to $r_{\lambda,X}$ and $r_{\chi,X}$ for λ^{XY} and χ^{XY} . These particles are out of the reach of the LHC, so we need a collider with larger energies to discover them. We find from the figure that the fermionic partner λ^{XY} , which may be called the *xyino*, is within the reach of the VLHC with center-of-mass energies of $(50 \sim 200)$ TeV for $r_{\lambda,X} \lesssim 1$. However, the discovery of the scalar partner χ^{XY} , or *sxyon*, may be difficult even at the VLHC with highest possible energies.

4.4 Xyon decay

Experimental properties of xyons depend strongly on their lifetime and/or decay modes. We here study xyon decay in general theories, including the holographic theories discussed in the previous two subsections.

Let us first consider the case where the DSB gauge interaction is asymptotically free (this is *not* the case in the holographic theories discussed before). In this case xyons φ arise as composite particles at the dynamical scale $\Lambda \approx (10 \sim 100)$ TeV. Now, let us introduce a composite chiral superfield Σ that contains xyons as the imaginary part of the lowest component, $\Sigma = (\chi + i\varphi) + \dots$. Since xyons are (pseudo-)Goldstone bosons, the dynamics of the DSB sector respect the shift symmetry $\Sigma \rightarrow \Sigma + i\epsilon$ where ϵ is a constant. Now, imagine that xyons are composed of n constituent fields, collectively denoted as \mathcal{Q} , so that $\Sigma \approx \mathcal{Q}^n/\Lambda^{n-1}$ ($n \geq 2$). Then the direct decay of xyons into the MSSM particles can be caused by interactions of the form $\mathcal{L} \approx \int d^4\theta \mathcal{Q}^n U^\dagger Q/M_*^n$, $\int d^4\theta \mathcal{Q}^n Q^\dagger E/M_*^n$ and $\int d^4\theta \mathcal{Q}^n L^\dagger D/M_*^n$. Here, M_* is the fundamental scale of the theory, expected to be of order the unification or Planck scale, and we have supplied powers of M_* by dimensional analysis. The dimension of \mathcal{Q} is counted as 1 (the canonical dimension), since the DSB gauge interaction is weak at the scale M_* by assumption. After confinement at the scale Λ , the interactions listed above lead to the effective operators $\mathcal{L} \sim \int d^4\theta (\Sigma + \Sigma^\dagger) U^\dagger Q$, $\int d^4\theta (\Sigma + \Sigma^\dagger) Q^\dagger E$ and $\int d^4\theta (\Sigma + \Sigma^\dagger) L^\dagger D$ with coefficients of order Λ^{n-1}/M_*^n . This gives the decay rate $\Gamma = O(m_\varphi^3 (\Lambda^{n-1}/M_*^n)^2 (m_q/m_\varphi)^2)$, where m_q is the largest mass of the final state fermions, leading to the lifetime of order $10^{-23} (M_*/\Lambda)^{2n}$ sec (here we have used $m_q = m_t$).¹⁵ If these are the dominant decay modes, therefore, the lifetime of xyons are much longer than the age of the universe, $\tau_\varphi \gg 10^{10}$ years.

It is possible that xyons have faster decay modes, depending on the spectrum of the DSB sector. Suppose that DSB gauge interactions produce composite states ϕ_A and ϕ_B , and that xyons can be converted into these states due to strong interactions of the DSB sector: $\varphi \rightarrow \phi_A + \phi_B$. The (virtual) states ϕ_A and ϕ_B can then directly decay into the MSSM particles, depending on their 321 gauge quantum numbers. For example, if ϕ_A and ϕ_B have the quantum numbers of L and D^\dagger , respectively, they can decay into the MSSM states through operators of the form $\mathcal{L} \sim \int d^2\theta L \bar{\Phi}_A$ and $\int d^2\theta D \Phi_B$, where $\bar{\Phi}_A$ and Φ_B are chiral superfields containing appropriate components of the massive ϕ_A and ϕ_B supermultiplets. Then, if $\bar{\Phi}_A$ and Φ_B are made out of n_A and n_B constituent fields ($n_A, n_B \geq 2$), the decay rate of xyons will be roughly of order $\Lambda (\Lambda/M_*)^{n_A+n_B-4}$, which could be much faster than the direct decay discussed before.

The situation is similar in the holographic theories, except that in this case interactions of the DSB sector do not become weak in the UV so that the dimensions of the composite operators, such as n_A and n_B above, are now free parameters taking arbitrary values larger than 1 (not necessarily integers due to large anomalous dimensions). In the 5D viewpoint, the direct decay

¹⁵For light final-state fermions, the decay into scalar superpartners can be faster with the rate given by $\Gamma = O(m_\varphi^3 (\Lambda^{n-1}/M_*^n)^2 \{(m_1^2 - m_2^2)/m_\varphi^2\}^2)$, where m_1 and m_2 are the masses of the two final-state scalars.

operators discussed before correspond to UV-brane operators of the form:

$$S_{\varphi,1} \sim \int d^4x \int_0^{\pi R} dy 2\delta(y) \left[\frac{1}{M_*} \int d^4\theta U^\dagger \mathcal{P}'[\mathcal{B}]Q + \frac{1}{M_*} \int d^4\theta Q^\dagger \mathcal{P}'[\mathcal{B}]E + \frac{1}{M_*} \int d^4\theta L^\dagger \mathcal{P}'[\mathcal{B}]D + \text{h.c.} \right], \quad (36)$$

where $\mathcal{B} \equiv \partial_y e^{2V} - \sqrt{2} \Sigma^\dagger e^{2V} - \sqrt{2} e^{2V} \Sigma$, and $\mathcal{P}'[\mathcal{X}]$ is a projection operator extracting the $(\mathbf{3}, \mathbf{2})_{-5/6}$ component of an $SU(5)$ adjoint \mathcal{X} (here we have suppressed order one coefficients). Since the wavefunction value of the canonically normalized xyon field is about $\sqrt{g_5^2 k} e^{-\pi k R} \approx \sqrt{\pi k R} (k'/k)$ at $y = 0$, this leads to the xyon decay rate $\Gamma \simeq (m_\varphi^3/8\pi)(\pi k R)(k'/k M_*)^2 (m_q/m_\varphi)^2 \sim m_\varphi^3 (k'/k^2)^2 (m_q/m_\varphi)^2$, which implies that the dimension of the composite xyon field is given by $n = 2$. In fact, this statement is generally true in any theories where xyons are identified as the extra dimensional component of the broken unified gauge bosons. We thus conclude that direct decays of xyons into the MSSM states are highly suppressed, leading to a lifetime much longer than the age of the universe if they are dominant decay modes.

Faster decay modes of xyons can, in principle, be available if some of the MSSM Higgs and/or matter fields propagate in the 5D bulk. In the case that only the Higgs fields propagate in the bulk, xyon decay could occur as follows. First, xyons can be converted into the MSSM Higgs-doublet and the (virtual) Higgs triplet states through the bulk gauge interaction, $S = \int d^4x \int dy \{-e^{-3k|y|} \int d^2\theta \sqrt{2} H^c \Sigma H + \text{h.c.}\}$, as $\varphi \rightarrow H_D + H_T^c$ (or $\varphi \rightarrow \bar{H}_D + \bar{H}_T^c$ through the corresponding interaction for $\{\bar{H}, \bar{H}^c\}$). The Higgs triplet state can then decay into the MSSM particles, for example through the UV-brane operators $S = \int d^4x \int dy 2\delta(y) \{(1/M_*) \int d^2\theta (\nabla_y H_T) Q Q + (1/M_*) \int d^2\theta (\nabla_y H_T) U E + \text{h.c.}\}$, where $\nabla_y H_T$ represents the triplet component of $\nabla_y H \equiv \partial_y H + \sqrt{2} \Sigma H$.¹⁶ This leads to a partial decay rate of xyons of order $\Gamma \approx k' (k'/k)^{4c_H+2}$, where c_H is the bulk mass parameter for the Higgs multiplet which controls the wavefunction profile for the zero mode (for details see [3]). Given that the successful prediction for gauge coupling unification requires $c_H \geq 1/2$ [3], we find that this decay mode cannot be much faster than the direct decay discussed before. We thus conclude that *if matter fields are localized on the UV brane, which is practically equivalent to the condition that the entire DSB sector is even under R parity, then xyons behave as stable particles at least for collider purposes.*

It is possible to consider the case where xyons decay much faster. This occurs if some of the MSSM matter fields propagate in the bulk. Suppose that D and L of the MSSM come from bulk hypermultiplets as follows. We introduce two hypermultiplets $\{F, F^c\}$ and $\{F', F'^c\}$ for each

¹⁶Possible operators such as $S = \int d^4x \int dy 2\delta(y) \{\int d^2\theta H_T^c Q L + \int d^2\theta H_T^c U D + \text{h.c.}\}$ are forbidden if we impose a continuous $U(1)_R$ symmetry with the charges $Q_R(V, \Sigma, H, \bar{H}) = 0$, $Q_R(H^c, \bar{H}^c) = 2$ and $Q_R(Q, U, D, L, E, N) = 1$, which is well motivated to provide complete solutions to the doublet-triplet and dimension-five proton decay problems [27]. These operators are allowed if we do not impose $U(1)_R$. Operators involving H_T without the y -derivative, e.g. $S = \int d^4x \int dy 2\delta(y) \{\int d^2\theta H_T Q Q + \int d^2\theta H_T U E + \text{h.c.}\}$, could also be allowed if the $SU(5)$ breaking on the UV brane is due to the Higgs mechanism. These operators would lead to faster decays with rates $\Gamma \approx k' (k'/k)^{4c_H}$. This, however, does not change our main conclusion here.

generation, transforming as $\mathbf{5}^*$ under $SU(5)$. By assigning suitable boundary conditions, it is possible to obtain four zero-mode states $D(\mathbf{3}^*, \mathbf{1})_{1/3} \subset F$, $L(\mathbf{1}, \mathbf{2})_{-1/2} \subset F'$, $L^c(\mathbf{1}, \mathbf{2})_{1/2} \subset F^c$ and $D^c(\mathbf{3}, \mathbf{1})_{-1/3} \subset F'^c$ from these two hypermultiplets. We then introduce two chiral superfields $D'(\mathbf{3}^*, \mathbf{1})_{1/3}$ and $L'(\mathbf{1}, \mathbf{2})_{-1/2}$ on the IR brane (for each generation) together with mass terms of the form $S = \int d^4x \int dy 2\delta(y - \pi R) \{ \int d^2\theta (DD^c + D'D^c + LL^c + L'L^c) + \text{h.c.} \}$. This leaves three generations of D and L at low energies, giving a complete matter sector of the MSSM together with the Q , U and E fields located on the UV brane. The bulk mass parameters of the $\{F, F^c\}$ and $\{F', F'^c\}$ fields are taken as $c_F, c_{F'} \geq 1/2$ to preserve the successful prediction for gauge coupling unification.¹⁷ An interesting feature of this setup is that we can arrange the theory such that it does not lead to proton decay at a rate inconsistent with experiments even without imposing an ad hoc symmetry. This occurs, for example, if the theory possesses a $U(1)_R$ symmetry of [27] and its breaking is encoded only in the F -component VEV of the supersymmetry-breaking field Z , or simply if only one or two generations are significantly delocalized from the UV brane. Potentially dangerous flavor changing neutral currents arising from the IR-brane mass mixings are suppressed sufficiently for $c_F, c_{F'} \geq 1/2$. To avoid reintroduction of the supersymmetric flavor problem, however, we need $c_F, c_{F'} \gtrsim 0.8$, unless we introduce an additional ingredient into the theory, such as a flavor symmetry in the bulk and on the IR brane together with appreciable tree-level UV-brane kinetic terms for bulk matter.

Xyon decay in the bulk matter theory discussed above occurs through the IR-brane operator

$$S_{\varphi,2} \sim \int d^4x \int_0^{\pi R} dy 2\delta(y - \pi R) \left[e^{-2\pi k R} \frac{1}{M_*^2} \int d^4\theta L^\dagger \mathcal{P}'[\mathcal{B}]D + \text{h.c.} \right], \quad (37)$$

where we have suppressed order one coefficients. This leads to the xyon decay interactions of the form

$$\mathcal{L}_{4D} \sim \xi \left((\partial_\mu \varphi) d^\alpha \sigma_{\alpha\dot{\alpha}}^\mu l^{\dot{\alpha}} - i(\partial_\mu \varphi) \{ \tilde{l}^* (\partial^\mu \tilde{q}) - (\partial^\mu \tilde{l}^*) \tilde{q} \} \right) + \text{h.c.}, \quad (38)$$

where φ is the xyon field transforming as $(\mathbf{3}, \mathbf{2})_{-5/6}$ under 321, and d , l , \tilde{d} and \tilde{l} are the down-type quark, doublet lepton, right-handed down-type squark and left-handed slepton, respectively. The coefficient ξ is given by

$$\xi \simeq \sqrt{\frac{(2c_F - 1)(2c_{F'} - 1)g_5^2 k}{(1 - e^{(1-2c_F)\pi k R})(1 - e^{(1-2c_{F'}\pi k R)}}} \left(\frac{k'}{M_*^2} \right) e^{-(c_F + c_{F'} - 1)\pi k R}, \quad (39)$$

where $M'_* \equiv M_* e^{-\pi k R}$, and this can be approximated further as

$$\xi \simeq \begin{cases} (1/\sqrt{\pi k R})(k'/M_*^2) & (\text{for } c_F, c_{F'} \simeq 1/2) \\ \sqrt{\pi k R} (k'/M_*^2) e^{-(c_F + c_{F'} - 1)\pi k R} & (\text{for } c_F, c_{F'} \gg 1/2). \end{cases} \quad (40)$$

¹⁷The successful prediction is not destroyed even for $c_F, c_{F'} < 1/2$, if for some reason $c_F = c_{F'}$.

The partial decay rates for xyons are given by

$$\Gamma_{\varphi \rightarrow d+l} \simeq \frac{\xi^2}{8\pi} (m_d^2 + m_l^2) m_\varphi, \quad (41)$$

for $\varphi \rightarrow d+l$ and

$$\Gamma_{\varphi \rightarrow \tilde{d}+\tilde{l}} \simeq \frac{\xi^2}{8\pi} \frac{(m_{\tilde{d}}^2 - m_{\tilde{l}}^2)^2}{m_\varphi}, \quad (42)$$

for $\varphi \rightarrow \tilde{d}+\tilde{l}$, where we have set $m_d, m_l, m_{\tilde{d}}, m_{\tilde{l}} \ll m_\varphi$. For the superparticle spectrum given in Eqs. (33 – 35) (and thus the parameters of Eqs. (32)) and $m_d = m_b$, we find that the dominant decay mode is that to a squark and a slepton. For $m_\varphi \simeq (2 \sim 3)$ TeV, the lifetime of xyons is given by

$$\tau_\varphi \simeq \begin{cases} 10^{-16} \text{ sec} & (\text{for } c_F, c_{F'} \simeq 1/2) \\ 10^{-19} \times e^{2(c_F+c_{F'}-1)\pi k R} \text{ sec} & (\text{for } c_F, c_{F'} \gg 1/2). \end{cases} \quad (43)$$

The shortest lifetime is obtained for $c_F = c_{F'} = 1/2$. Note that even for $c_F = c_{F'} = 1/2$ the lifetime is long enough such that $\Gamma_\varphi/m_\varphi \ll 1$. Therefore, we conclude that *the xyon always appears as a narrow particle rather than a broad resonance*. The lifetime of xyons becomes exponentially longer for larger values of c_F and $c_{F'}$. For example, the lifetime is already of order $\tau_\varphi \approx 10^{-4}$ sec for $c_F = c_{F'} = 0.8$.

A final comment is in order. We have implicitly assumed in our analysis that there are no light exotic particles, for example colored Higgs fields, into which xyons can decay. This is a reasonable assumption because if the parameters of the theory obey naive dimensional analysis the masses of these exotic particles are of order $\pi k'$, which are much larger than the xyon mass. If the masses of the exotic particles are somehow small, however, phenomenology of xyons (and the exotic particles) could change significantly. We will not pursue such a possibility further in this paper.

5 Experimental Signatures

In this section we study experimental signatures of xyons. We first study signals and reaches of xyons at hadron colliders. We then discuss possible indirect effects of xyons in the case that the xyon mass lies in the range outside of the direct reach of the LHC. We also discuss cosmological implications of our scenario.

5.1 Collider search

Since xyons are generally colored, they hadronize after production, picking up the standard model quarks. Here we mainly consider the case where xyons are long lived (the case where

matter fields are localized on or towards the UV brane in the holographic 5D theories) and study experimental consequences of having these exotic hadrons.

In the simplest case of $SU(5)$ xyons, the 321 quantum numbers of xyons are given by $(\mathbf{3}, \mathbf{2})_{-5/6}$. Let us denote the isospin up and down components of the $(\mathbf{3}, \mathbf{2})_{-5/6}$ xyon as φ_\uparrow and φ_\downarrow , respectively. We first find that the contributions from the $SU(2)_L$ and $U(1)_Y$ D -terms to the xyon squared masses, $\delta m_{D,\varphi}^2$, are only of order $O(m_Z^4/(\pi k')^2)$: $\delta m_{D,\varphi_\uparrow}^2 - \delta m_{D,\varphi_\downarrow}^2 \simeq -(5/16)(m_Z^4/m_{\chi_{XY}}^2) \cos^2 2\beta$, where $\tan \beta$ is the ratio of the VEVs of the two Higgs doublets. This is because the auxiliary fields D couple in the Lagrangian only in the form $\mathcal{L} \sim \chi^{XY} D^{321} A_5^{XY}$ (see Appendix A). This implies that the contributions to the mass splitting $m_{\varphi_\uparrow} - m_{\varphi_\downarrow}$ from the D -terms are negligible.

The dominant effect for the mass splitting between φ_\uparrow and φ_\downarrow then arises from loops of the gauge fields. The effect comes dominantly from one loop of the electroweak gauge bosons with the loop momenta of order m_φ , giving the mass splitting $m_{\varphi_\uparrow} - m_{\varphi_\downarrow} \simeq 2\pi(Q_\uparrow^2 - Q_\downarrow^2)(e^2/16\pi^2)m_Z$. Here, $Q_\uparrow = -1/3$ and $Q_\downarrow = -4/3$ are the electric charges of φ_\uparrow and φ_\downarrow , respectively. This gives the mass splitting $m_{\varphi_\uparrow} - m_{\varphi_\downarrow} \simeq -600$ MeV. While a mass splitting of this size is not negligible, we find it useful to classify the hadronic states consisting of xyons and the light quarks, u and d , using an approximate $SU(2)_\varphi \times SU(2)_q$ symmetry, where φ_\uparrow and φ_\downarrow form a doublet under $SU(2)_\varphi$ while u and d a doublet under $SU(2)_q$. We then find that in a given $SU(2)_\varphi \times SU(2)_q$ multiplet the states containing φ_\uparrow are lighter than those containing φ_\downarrow by about 600 MeV.

The lightest xyonic hadrons are expected to be one of the four fermionic mesons

$$\tilde{T}^0 \equiv \varphi_\uparrow \bar{d}, \quad \tilde{T}^- \equiv \varphi_\uparrow \bar{u}, \quad \tilde{T}'^- \equiv \varphi_\downarrow \bar{d}, \quad \tilde{T}'^{--} \equiv \varphi_\downarrow \bar{u}, \quad (44)$$

which form a $(\mathbf{2}, \mathbf{2})$ multiplet under $SU(2)_\varphi \times SU(2)_q$. Here, the superscripts represent the electric charges. As we have seen, the masses of these xyonic mesons (*xymesons*) split due to the mass difference between φ_\uparrow and φ_\downarrow — xymesons containing φ_\downarrow are heavier than those containing φ_\uparrow by about 600 MeV. This implies that \tilde{T}'^- (\tilde{T}'^{--}) decays into \tilde{T}^0 (\tilde{T}^-) and a charged pion with the lifetime of about 10^{-12} sec. The mass splitting between \tilde{T}^0 and \tilde{T}^- (and \tilde{T}'^- and \tilde{T}'^{--}) is of order a few MeV, which comes from isospin breaking effects due to electromagnetic interactions and the u - d mass difference. Because the two effects work in the opposite direction, it is not clear which of \tilde{T}^0 and \tilde{T}^- is lighter. While the heavier one decays into the lighter one and leptons through weak interactions, its lifetime is of order 10^{-1} to 10^2 seconds, so that both \tilde{T}^0 and \tilde{T}^- are essentially stable for collider purposes.

There are also bosonic baryons formed by xyons and the standard model quarks. The lightest states of these xyonic baryons (*xybaryons*) will come either from a $(\mathbf{2}, \mathbf{1})$ scalar multiplet

$$\tilde{U}_S^0 \equiv \varphi_\uparrow [ud], \quad \tilde{U}_S^- \equiv \varphi_\downarrow [ud], \quad (45)$$

or from a $(\mathbf{2}, \mathbf{3})$ vector multiplet

$$\begin{aligned} \tilde{U}_V^+ &\equiv \varphi_\uparrow uu, & \tilde{U}_V^0 &\equiv \varphi_\uparrow \{ud\}, & \tilde{U}_V^- &\equiv \varphi_\uparrow dd, \\ \tilde{U}_V'^0 &\equiv \varphi_\downarrow uu, & \tilde{U}_V'^- &\equiv \varphi_\downarrow \{ud\}, & \tilde{U}_V'^-- &\equiv \varphi_\downarrow dd. \end{aligned} \quad (46)$$

Here, $\{\}$ and $[\]$ denote symmetrization and antisymmetrization, respectively, and scalar and vector multiplets have spin-0 and spin-1, respectively. Because of the φ_\uparrow - φ_\downarrow mass difference, \tilde{U}_S^- ($\{\tilde{U}_V'^0, \tilde{U}_V'^-, \tilde{U}_V'^--\}$) is heavier than \tilde{U}_S^0 ($\{\tilde{U}_V^+, \tilde{U}_V^0, \tilde{U}_V^-\}$) by about 600 MeV. The mass splittings among \tilde{U}_V^+ , \tilde{U}_V^0 and \tilde{U}_V^- (and $\tilde{U}_V'^0$, $\tilde{U}_V'^-$ and $\tilde{U}_V'^--$) are of order a few MeV, arising from isospin breaking effects. Finally, the mass splitting between particles in the $(\mathbf{2}, \mathbf{1})$ multiplet and those in the $(\mathbf{2}, \mathbf{3})$ multiplet arises from spin-dependent interactions, which is expected to be a few hundred MeV. Thus, the heavier will decay into the lighter and pions by strong interactions. This implies that only the lighter of \tilde{U}_S^0 and $\{\tilde{U}_V^+, \tilde{U}_V^0, \tilde{U}_V^-\}$ behaves as a stable particle(s) at colliders. The stability of the lighter is ensured by baryon number conservation (unless the mass of the lightest xybaryon is larger than the sum of the nucleon and the lightest xymeson masses, which we think is unlikely). The naive nonrelativistic quark model suggests that \tilde{U}_S^0 is lighter. The mass splitting between the lightest xybaryons and xymesons are expected to be of order a few hundred MeV.

In fact, we can work out the spectrum of the lightest xyhadrons in more detail, if we apply the empirical mass formula for the lowest-lying hadronic states with no radial excitation or orbital angular momentum [33]. We expect that the masses of the φ_\uparrow -xyhadron states $\{\tilde{T}^0, \tilde{T}^-\}$, \tilde{U}_S^0 and $\{\tilde{U}_V^+, \tilde{U}_V^0, \tilde{U}_V^-\}$ are roughly given by $m_{\varphi_\uparrow} + (300 \text{ MeV})$, $m_{\varphi_\uparrow} + (460 \text{ MeV})$ and $m_{\varphi_\uparrow} + (650 \text{ MeV})$, respectively, with the mass splittings among the states inside a curly bracket of order a few MeV. This spectrum ensures the stability of the lightest xybaryon and allows a vector xybaryon to decay into a scalar xybaryon and a pion through strong interactions. A similar pattern is repeated for the xyhadrons containing φ_\downarrow : the masses of $\{\tilde{T}'^-, \tilde{T}'--\}$, \tilde{U}_S^- and $\{\tilde{U}_V'^0, \tilde{U}_V'^-, \tilde{U}_V'^--\}$ are roughly given by $m_{\varphi_\downarrow} + (300 \text{ MeV})$, $m_{\varphi_\downarrow} + (460 \text{ MeV})$, and $m_{\varphi_\downarrow} + (650 \text{ MeV})$, with the mass splittings among the states inside a curly bracket again of order a few MeV. Here, $m_{\varphi_\downarrow} \simeq m_{\varphi_\uparrow} + (600 \text{ MeV})$.

Now, let us consider signals of these xyhadronic states at hadron colliders. Since both of the two lightest xymesons, \tilde{T}^0 and \tilde{T}^- , as well as the lightest xybaryon (presumably \tilde{U}_S^0) are effectively stable, we have both neutral and charged stable heavy particles at colliders. While all these particles undergo hadronic interactions in the detectors, neutral ones are difficult to see in practice (although they may be seen as intermittent highly ionizing tracks through isospin and charge exchange with background material). On the other hand, charged particles leave highly ionizing tracks both in the inner tracking region and the outer muon system, so that they can be detected relatively easily. In fact, these signals are quite common in warped unified theories [27], which often lead to stable colored particles at colliders. The production of these particles occurs

through strong interaction processes, and the reach in their masses is roughly 2 TeV at the LHC.

A more precise estimate for the reach in xyon masses can be obtained from a detailed study of the hadronic production of colored particles given in Ref. [34]. Here we require that charged stable xyhadrons reach the outer muon system to be observed, which gives conservative estimates for the reach in xyon mass. We also assume, for simplicity, that all the produced xyons hadronize into xymesons, although we expect that the estimates are not much affected if some (presumably small) fraction of xyons hadronizes into xybaryons. In the case of $SU(5)$ xyons, this implies that roughly 1/2 of the produced xyons hadronize into charged particles that can be detected in both the inner and outer systems. Here, we have assumed that xyhadrons in a single $SU(2)_q$ multiplet are produced with an almost equal probability in hadronization processes. Since the signals of highly ionizing tracks caused by massive charged particles are almost background free, the reach is essentially determined by the production rate. If we require the observation of 4 (10) events for the “discovery” of xyons, we find that the reach in xyon masses is about 1.8, 2.0 and 2.2 TeV (1.6, 1.8 and 2.0 TeV) at the LHC with integrated luminosity of 100, 300 and 1000 fb^{-1} , respectively. Comparing with the theoretically expected range for the xyon mass given in Fig. 4, we find that xyons may be observed at the LHC if the parameter $r_{\lambda,i}$ takes values somewhat smaller than unity, e.g. $r_{\lambda,i} \lesssim 0.5$.

The discovery of xyons at the VLHC is much more promising. Requiring 10 events for the discovery, we find that the VLHC with a center-of-mass energy of 50 TeV (200 TeV) has a reach in xyon masses of about 3.7, 4.3 and 5.0 TeV (9.0, 11 and 13 TeV) for integrated luminosity of 100, 300 and 1000 fb^{-1} , respectively. Given the fact that the xyon mass saturates for large $r_{\lambda,i}$ for a fixed value of k' (see Fig. 4), we find that the VLHC with a center-of-mass energy of 50 TeV (200 TeV) can cover the entire parameter region of $r_{\lambda,i}$ for $k' \lesssim 13$ TeV (33 TeV). Since we naturally expect $k' \approx 10$ TeV (to obtain weak-scale superparticle masses with all the parameters obeying naive dimensional analysis; see subsection 4.3), the discovery of xyons at the VLHC is quite promising.¹⁸

There may also be other signals that can be used to detect xyons. When antixymesons or xybaryons traverse a detector, they may exchange isospin and charge with the background material through hadronic interactions, and so may make transitions between neutral and charged states. This leaves a distinct signature of intermittent highly ionizing tracks. Neutral xyhadrons also give a signature of jets plus transverse missing energy, which may be observed at the VLHC. If xyons pick up strange quarks after their production, they form strange xyhadrons. These xyhadrons are expected to be heavier than non-strange xyhadrons by about 100 MeV, so that the lightest strange xymeson (or xybaryon) decays into a non-strange one through weak interactions.

¹⁸If the 321 gauge couplings are weak at the unification scale, as can be the case in the holographic theories with $SU(5)$ broken by the Higgs mechanism on the UV brane, k' can be larger but only by a factor of two or so.

Assuming that the mass difference is smaller than the pion mass, the lifetime of the decay will be of order $10^{-8} \sim 10^{-7}$ sec with the final state containing leptons (otherwise it will be of order $10^{-12} \sim 10^{-10}$ sec with a charged pion in the final state). Since the decay could change the charges of the xyhadronic states, these xyhadrons may leave tracks in the inner tracking region but not in the outer muon system, or vice versa.

Testing the $SU(2)_L$ -doublet nature of xyons will not be easy. One possibility might be to use the decay of φ_{\downarrow} into φ_{\uparrow} . As we have seen, a xyhadron containing φ_{\downarrow} is heavier than the one with φ_{\downarrow} replaced by φ_{\uparrow} , by about 600 MeV. This implies that some xyhadrons, for example \tilde{T}'^- , \tilde{T}'^{--} and \tilde{U}_S^- , decay through weak interactions with the lifetime of about 10^{-12} sec, corresponding to the decay length of about sub-millimeters. The final state contains either a charged or neutral xyhadron and a charged pion. Therefore, if one could somehow see the final-state xyhadrons and the soft charged pions, arising from decays of pair-produced xyons, and determine the decay points precisely, one might be able to see the $SU(2)_L$ -doublet nature of xyons.

We finally consider the case in which the lightest xyon, φ_{\uparrow} , is unstable at a collider timescale, as in the case of the holographic theories with matter fields propagating in the bulk. In this case, xyhadrons may decay into the MSSM particles inside the detector. In particular, the lightest xymeson and xybaryon can also decay inside the detector. The lifetime is highly sensitive to the parameters of the theory. While we naturally expect that it is still longer than about 10^{-4} sec to avoid reintroduction of the supersymmetric flavor problem, it can in principle be any number larger than about 10^{-16} sec. The decay products will consist of an energetic (s)quark and an energetic (s)lepton. This, therefore, potentially provides a distinct signature at hadron colliders.

5.2 Super-oblique corrections

Since the xyon supermultiplet has large mass splittings among its components, it can potentially leave non-negligible effects on some parameters at energies lower than the xyon mass. These effects could become important if xyons are so heavy that they cannot be directly produced at the LHC. Here we briefly discuss these effects and estimate their sizes. We find, unfortunately, that they are not large and thus cannot be used to probe xyons indirectly.

Consider a generic supermultiplet charged under some gauge group. If this multiplet has large mass splittings among its components, then it induces a difference between the couplings of the gauge boson and the gaugino at loop level. This type of correction is called a super-oblique correction, which does not decouple as the multiplet gets heavy as long as the fractional mass differences among the components stay the same [35]. At the leading-log level, the corrections are estimated using the renormalization group equations for the gauge and gaugino couplings, which are equal in the supersymmetric limit but not if supersymmetry is broken. In the case of $SU(5)$ xyons, we find that the differences between the gauge coupling g_i and the gaugino

coupling \tilde{g}_i at a scale below the xyon mass are given by

$$\tilde{U}_i \equiv \frac{\tilde{g}_i}{g_i} - 1 \simeq \frac{g_i^2 \hat{b}_i}{16\pi^2} \ln \frac{M_{\tilde{\varphi}}}{m_{\varphi}}, \quad (47)$$

where $(\hat{b}_1, \hat{b}_2, \hat{b}_3) = (5/6, 1/2, 1/3)$, $i = 1, 2, 3$ represents $U(1)_Y$, $SU(2)_L$ and $SU(3)_C$, respectively, and $M_{\tilde{\varphi}}$ is the mass scale for the superpartners of xyons, $\tilde{\varphi} = \lambda'^{XY}, \chi^{XY}$. Since $\ln(M_{\tilde{\varphi}}/m_{\varphi}) \approx 2$, we find that the corrections are not large — for example, $(\tilde{U}_1, \tilde{U}_2, \tilde{U}_3) = (0.23\%, 0.27\%, 0.48\%)$ for $\ln(M_{\tilde{\varphi}}/m_{\varphi}) = 2$. We obtain somewhat larger corrections for xyons associated with the IR breaking of $SO(10) \rightarrow SU(4)_C \times SU(2)_L \times SU(2)_R$: $(\hat{b}_1, \hat{b}_2, \hat{b}_3) = (13/15, 1, 2/3)$ and $(\tilde{U}_1, \tilde{U}_2, \tilde{U}_3) = (0.24\%, 0.54\%, 0.97\%)$ for $\ln(M_{\tilde{\varphi}}/m_{\varphi}) = 2$, but these are still small. In fact, corrections of these sizes are expected to arise generically as threshold corrections from the DSB sector. For example, IR-brane operators of the form $\mathcal{L} \approx 2\delta(y - \pi R) \int d^4\theta Z^\dagger Z (\mathcal{W}_i^\alpha \mathcal{D}^2 \mathcal{W}_{i\alpha} + \text{h.c.})$ naturally give contributions to \tilde{U}_i comparable to those from xyons. Therefore, we find it is difficult to use super-oblique corrections to probe xyons indirectly when they are not produced at colliders.

The smallness of the xyon contributions to \tilde{U}_i is generic, because it mainly comes from the fact that xyons are scalars and thus do not contribute significantly to the group-theoretical factors \hat{b}_i . It is also generically true that the mass splittings in the xyon supermultiplet are not very large, i.e. $\ln(M_{\tilde{\varphi}}/m_{\varphi})$ is not very large, and that the multiplicity of xyon supermultiplets is not very large either.

5.3 Cosmology

Cosmological implications of xyons depend very much on their lifetime. We first consider the case in which the lifetime of xyons is much longer than the age of the universe. Assuming that the thermal history of the universe is standard below the temperature of about 10 TeV, the relic abundance of xyonic particles (xyhadrons) today are estimated as follows. Below the temperature of about $T \simeq m_{\varphi}/28 \approx 100$ GeV, annihilation of xyons into gluons becomes ineffective and the xyon abundance freezes out. If there is no subsequent annihilation of xyons, this will lead to the present xyon energy density of about $\Omega_{\varphi} \simeq (0.01 \sim 1)$ for $m_{\varphi} \simeq (1 \sim 10)$ TeV. However, there may be periods of further annihilations at later stages in the evolution of the universe, which could significantly reduce Ω_{φ} . The most important among these would come from nonperturbative QCD effects at a temperature of about $T \simeq \Lambda_{\text{QCD}} \approx 300$ MeV.

At $T \simeq \Lambda_{\text{QCD}}$, xyons will hadronize into xyhadrons. The annihilation cross sections of these xyhadrons are difficult to estimate because they are determined by nonperturbative QCD effects. The largest possible cross section, which leads to the smallest relic abundance, will result if it is the same order as the nucleon-nucleon cross sections at low energies, $\sigma_{\text{ann.}} \sim (m_{\pi}^2 \beta)^{-1}$, where m_{π} is the pion mass and β the relative velocity between the two xyhadrons. Since nucleon-nucleon

scatterings at low energies are mostly quark rearrangement processes, it is not clear if the xyon annihilation cross section, which requires annihilation of xyon cores, takes a value similar to that of the low-energy nucleon-nucleon cross sections. However, it may be possible that, when two xyhadrons approach, they form a bound state (xynuclei) with a cross section of order $(m_\pi^2\beta)^{-1}$, and then this bound state reorganizes itself into $\varphi\bar{\varphi}$ and the usual hadrons for energetic reasons, leading to rapid xyon annihilation. If this happens, the xyon annihilation cross section is, in fact, given by $\sigma_{\text{ann.}} \sim (m_\pi^2\beta)^{-1}$, leading to a very small abundance of $\Omega_\varphi \simeq 10^{-10}$ [36]. Since we do not really know the low-energy dynamics of xyhadrons, the estimate of the xyon relic abundance is subject to a rather large uncertainty:

$$10^{-10} \lesssim \Omega_\varphi \lesssim 1. \quad (48)$$

Note that, if nonperturbative annihilation at the QCD era is effective, we generically expect the value of Ω_φ in the lower part of this range. For example, the relic abundance can be as small as $\Omega_\varphi \simeq 10^{-8}$ even for $\sigma_{\text{ann.}} \sim m_\pi^{-2}$ without the $1/\beta$ enhancement.

While there is a recent argument that the nonperturbative enhancement of annihilation at the QCD era is unlikely to occur [37], we first discuss observational constraints on xyons in the case that the relic abundance of xyons is given by the lower range of Eq. (48). For these small values for the abundance and the xyon mass range of our interest, most of the constraints from direct search experiments are satisfied [38]. Strong constraints, however, come from heavy isotope searches. For $1 \text{ TeV} \lesssim m_\varphi \lesssim 10 \text{ TeV}$, the relevant bounds are those in Ref. [39].¹⁹ Some of the dark matter search experiments also give strong constraints. Implications of these bounds, however, differ depending on which of \tilde{T}^0 and \tilde{T}^- is the lightest xymeson.

In the case that \tilde{T}^- is the lightest xymeson, most of the relic xyons will be in the form of \tilde{T}^- with some of them in the form of the lightest xybaryon, \tilde{U}_g^0 . The charged xymeson, \tilde{T}^- , is then bound with a proton at the time of nucleosynthesis, while its antiparticle is bound with an electron at the recombination era [41]. At the time of galaxy formation, the antixymeson-electron bound state dissipates energy through radiation and collapses into the galactic disk. This implies that its local abundance around the earth will be enhanced compared with the cosmic abundance of Eq. (48) by about a factor of 10^7 or more. On the other hand, the local abundance of the xymeson-proton bound state is about 10^5 times the cosmic abundance, as it is determined purely by gravitational clusterings. With these local abundances, the bounds in [39], as well as data from plastic track detectors, exclude the existence of the stable charged xymeson. This case, therefore, will be viable only if there is a significant entropy production below the temperature of order TeV in the history of the universe.

¹⁹For $m_\varphi \lesssim 1 \text{ TeV}$, the strongest bound would come from that in Ref. [40].

What if the lightest xymeson is \tilde{T}^0 ? In this case, the relic xyons are mostly in the form of \tilde{T}^0 with a small fraction in the form of \tilde{U}_g^0 . The local xyon density is about 10^5 times the cosmic abundance of Eq. (48). With Ω_φ in the lower range of Eq. (48), most of the constraints from direct searches at balloon, satellite, ground- and underground-based experiments are satisfied (a roughly upper-half portion of the range of Eq. (48) could be excluded by the bounds from xyhadron annihilation in the halo [42].) The significant constraints, however, may come from heavy isotope searches and dark matter search experiments located at shallow sites.

Let us first consider the constraints from heavy isotope search experiments. Suppose now that the relic xyhadrons are bound in nuclei, forming anomalous heavy isotopes. Then the number density of these anomalous heavy xynuclei compared to that of the ordinary nuclei in the earth can be estimated from the expected xyhadron flux on the earth's surface as

$$r \sim 10^{-18} \Omega_\varphi \left(\frac{\text{TeV}}{m_\varphi} \right) \left(\frac{t_{\text{acc}}}{\text{yr}} \right), \quad (49)$$

where t_{acc} is the time period over which xynuclei accumulate in a sample of matter without being removed [43]. For the lowest possible value of $\Omega_\varphi \simeq 10^{-10}$ and a reasonable time period $t_{\text{acc}} \simeq (10^8 \sim 10^{10})$ yr, we obtain $r \sim (10^{-20} \sim 10^{-18})(\text{TeV}/m_\varphi)$. These values are marginally consistent with the bounds in [39], given the possibility of r being further reduced by a factor of 100 for hydrogen due to geochemical processes. There are also constraints from the amount of primordial heavy isotopes containing xyhadrons, generated during nucleosynthesis, which give $\Omega_\varphi \lesssim 10^{-7}$ [44].²⁰ Overall, the thermal xyon relics seem to be consistent with heavy isotope searches, but only if Ω_φ is in the lower edge of the region in Eq. (48). Note, however, that, in contrast with \tilde{T}^- , neutral xyhadrons \tilde{T}^0 and \tilde{U}_g^0 may not bind with ordinary matter to form heavy isotopes. While these particles feel the ordinary nuclear force, it is possible that they are not bound into nuclei, especially into lighter ones, for energetic reasons. If this is the case, the bounds from heavy isotope searches disappear.

The constraints on the xyon relic density also come from dark matter search experiments. Since xyhadrons are strongly interacting, their energies are significantly degraded during propagations in matter due to collisions, so they cannot reach deep underground. In order for an experiment to be able to constrain the xyon abundance, therefore, it must be located at a relatively shallow site, a depth smaller than about 100 meters of water equivalent. This almost singles out the relevant experiment to be the CDMS experiment at Stanford [45]. Assuming that the xyhadron-nuclei cross sections are given by the geometric cross sections of $\sigma \sim \pi A^{2/3} m_\pi^{-2}$, where A is the nucleon number of the target nucleus, we estimate that xyhadrons typically un-

²⁰The constraints on the lightest xymeson, which has isospin 1/2, may be different from those on a heavy colored particle with isospin 0, especially because the xymeson could bind with the proton due to one-pion exchange. We estimate, however, that the difference is not very large.

dergo ($30 \sim 40$) collisions before reaching the detector. A significant energy degradation, on the other hand, occurs only after about 100 or more collisions, implying that the CDMS detector can constrain the xyon relic abundance. By estimating the number of events expected from cosmic neutral xyhadrons and comparing it with the nuclear-recoil data, we find that the lower edge of the region in Eq. (48) may be marginally consistent with the data, but not for larger values. Given the crudeness of our estimate, we can consider that the thermal xyon relics are consistent with the data if $\Omega_\varphi \sim 10^{-10}$, although a more careful analysis will be need to be really conclusive.²¹

We have seen that the existence of stable xyons may be consistent with all the observations if the xyon relic abundance is as small as $\Omega_\varphi \sim 10^{-10}$ due to a large nonperturbative enhancement of the annihilation cross section at the QCD era. This enhancement, however, may not occur. In this case, there are essentially two ways to make cosmology consistent. One is to consider “non-standard” cosmology, such as a significant late-time entropy production below the temperature of about a TeV. The other is to consider the case where xyons are unstable. We here discuss the latter case. If the xyon lifetime is shorter than $\simeq 10^{-1}$ sec, xyons decay before nucleosynthesis and there is no cosmological constraint. In the case that the lifetime is longer than $\simeq 10^{-1}$ sec (and still shorter than the age of the universe), there are potential constraints coming, for example, from the destruction of the light nuclei synthesized during nucleosynthesis and the distortions of the diffuse gamma-ray background and the cosmic microwave background. In the case that the xyon relic abundance is determined by perturbative annihilation, $\Omega_\varphi \simeq (0.01 \sim 1)$ for $m_\varphi \simeq (1 \sim 10)$ TeV, these constraints require the lifetime of xyons to be shorter than about 100 sec [37]. Xyons with such lifetimes can naturally arise if matter fields propagate in the bulk in the holographic 5D theories ($c \lesssim 0.9$ if the relevant matter fields have the same bulk mass parameter). If the xyon lifetime is longer than 100 sec, the xyon relic density is constrained to be in the lower range of Eq. (48), although not necessarily at the lowest edge of $\Omega_\varphi \simeq 10^{-10}$.

In the case that the xyon lifetime is shorter than $\simeq 100$ sec or $\Omega_\varphi \simeq 10^{-10}$ with stable neutral xymesons, the thermal history of the universe can be standard. This opens up the possibility of having dark matter whose abundance is determined by conventional analyses. For example, dark matter may be the QCD axion with a decay constant of order $f_{\text{PQ}} \simeq 10^{12}$ GeV. A more attractive possibility will be a dark matter candidate whose interaction strengths are set by the TeV scale, because then the observed amount of dark matter is naturally reproduced. In fact, such a particle can arise naturally in our scenario from fields localized on the IR brane [26].²²

²¹If the cross sections between xyhadrons and nuclei are much larger than the geometric cross sections, e.g. by an order of magnitude or more, the constraint from CDMS will disappear as cosmic xyhadrons will not be able to reach the detector without significant energy degradations. The constraint also becomes weaker, if the cross sections are much smaller than the geometric ones, because the expected event rates then decreases.

²²An alternative possibility is the pedestrian dark matter discussed in [4], which can arise from the extended

Suppose we introduce a pair of singlet chiral superfields S and \bar{S} on the IR brane and introduce a vector-like symmetry acting (only) on them: either a $U(1)$ symmetry, $S(+1)$ and $\bar{S}(-1)$, or a Z_2 symmetry under which both S and \bar{S} are odd. The mass and interactions for these fields are then given by

$$S_{\text{DM}} = \int d^4x \int_0^{\pi R} dy 2\delta(y-\pi R) \left[e^{-2\pi k R} \int d^2\theta M_S S \bar{S} + \sum_{i=1,2,3} \int d^2\theta \frac{1}{M_i^2} S \bar{S} \text{Tr}[\mathcal{W}_i^\alpha \mathcal{W}_{i\alpha}] + \text{h.c.} \right], \quad (50)$$

where we have assumed, for simplicity, that S and \bar{S} carry $U(1)$ charges. Using naive dimensional analysis, we find $M_S \approx M_*$ and $M_i^2 \approx (M_*/\pi k)^3 k^2$. The mass splitting between the fermionic and bosonic components of S and \bar{S} comes from couplings of S and \bar{S} to the supersymmetry breaking field Z . Assuming that the fermionic component is the lightest, dark matter is a single Dirac fermion $\Psi = \{\psi_S, \psi_{\bar{S}}\}$, which annihilates into the MSSM gauginos through the four-Fermi operators suppressed by $M_i'^2 \equiv M_i^2 e^{-2\pi k R} \approx (M_*/\pi k)^3 k'^2$. The mass of this particle is close to the cutoff scale, $M_\Psi = M_S e^{-\pi k R} \approx M'_*$. The annihilation of Ψ occurs through the s -wave with the thermally averaged cross section given by $\langle \sigma v \rangle \approx (n/8\pi)(M_\Psi^2/M_i'^4)$, where n is the multiplicity of the final-state gauginos. Using the values $M_*/\pi k \approx 3$, $k' \approx 10$ TeV and $n \approx 10$, we obtain the relic Ψ abundance of $\Omega_\Psi \approx (0.1 \sim 1)$. In fact, the correct abundance is reproduced in a wide range of parameters with the dark matter mass of $M_\Psi \approx (10 \sim 100)$ TeV. From the 4D point of view, our dark matter Ψ is a stable composite state of the DSB sector [46], but with the important new ingredient that it “directly” couples to the MSSM states through mixings between the elementary states and the composite DSB states. Annihilation could also occur into the Higgs fields, if the Higgs doublets have nearly conformally-flat wavefunctions. The IR-brane dark matter may also be a Majorana fermion (no \bar{S} field). It is interesting that we are led to a picture of dark matter with a characteristic scale of $\approx (10 \sim 100)$ TeV, rather than the conventional one of $\approx (0.1 \sim 1)$ TeV.²³ Unfortunately, the direct detection of our IR-brane dark matter will be difficult because the cross sections with nuclei are suppressed by large mass parameters $M_i' = O(10 \sim 100 \text{ TeV})$.

It is interesting to note that the class of theories discussed here is free from dangerous relics such as the gravitino and moduli. Since the supersymmetry-breaking scale is very low, $\Lambda \approx (10 \sim 100)$ TeV, we expect that the gravitino (and moduli, if any) is very light $m_{3/2} \simeq \Lambda^2/M_{\text{Pl}} \approx (0.1 \sim 10)$ eV. In the particular context of the 5D theory discussed in subsection 4.2, we find

$$m_{3/2} \simeq \frac{\pi}{4\sqrt{3}} \left(\frac{M_*}{\pi k} \right)^2 \frac{k'^2}{M_{\text{Pl}}} \simeq 0.2 \left(\frac{M_*/\pi k}{3} \right)^2 \left(\frac{k'}{10 \text{ TeV}} \right)^2 \text{ eV}, \quad (51)$$

Higgs sector of the model.

²³The annihilation of such dark matter in the galactic center may provide the origin of the recently observed high-energy γ -ray flux from that region [47]. The high-energy γ -ray flux as a signal of dark matter annihilation has recently been considered in the context of the lightest messenger dark matter [48].

where we have used naive dimensional analysis to obtain $F_Z \simeq M_*^2/4\pi$. Such a light gravitino does not produce the “gravitino problem”, as its thermal relic abundance is small. It also evades the bound, $m_{3/2} \lesssim 16$ eV, recently derived from the analysis of the matter power spectrum and the cosmic microwave background data [49]. We note that in warped theories the radion does not cause any cosmological problem either, because its mass and interaction strengths are both dictated by the TeV scale, so that it decays before nucleosynthesis. These features allow the theory to have a high reheating temperature after inflation without contradicting with the observations. In particular, this implies that the theory may accommodate baryogenesis at high temperatures without any conflict. For example, assuming that there is no significant entropy production associated with the phase transition in the DSB sector (the viability of this assumption depends on the dynamics of the phase transition, especially the mechanism of radius stabilization [50]), the theory accommodates conventional thermal leptogenesis at the temperature $T \simeq 10^{10}$ GeV [51].²⁴

6 Discussion and Conclusions

In this paper we have argued that the requirement for the absence of fine-tuning in supersymmetric theories naturally leads to a class of theories that predicts exotic scalar particles with mass in the multi-TeV region. The key ingredients to evade fine-tuning in supersymmetric theories are the following:

- (1) There is an additional contribution(s) to the mass of the physical Higgs boson (to the Higgs quartic couplings) other than that from the $SU(2)_L \times U(1)_Y$ D -terms of the MSSM.
- (2) The mediation scale of supersymmetry breaking is low: $M_{\text{mess}} = O(10 \sim 100 \text{ TeV})$.
- (3) The masses of the squarks and sleptons do not respect the unified mass relations arising from the simple “ $SU(5)$ -symmetric” supersymmetry breaking sector.

To evade the fine-tuning, (i) is absolutely necessary. However, if we want to preserve one of the major successes of supersymmetry — the constraints from the precision electroweak data are satisfied relatively straightforwardly — then this is not enough. We need to satisfy (ii) and/or (iii), most likely both. In fact, for $M_{\text{Higgs}} \lesssim 250$ GeV as suggested by the data, the direct effect of raising the Higgs-boson mass to reduce fine-tuning, manifested as the increase of the left-hand-side of Eq. (1), is not so significant. Rather, the virtue of having the additional source of the Higgs quartic coupling lies in the fact that we do not need large top squark masses

²⁴The mechanism of soft leptogenesis has been discussed very recently in [52], which may work regardless of the entropy production if the right-handed neutrinos have Majorana masses of order ($1 \sim 10$) TeV and the temperature after the phase transition is as high as the right-handed neutrino masses.

to have large radiative corrections to the physical Higgs-boson mass to evade the experimental bound of $M_{\text{Higgs}} \gtrsim 114$ GeV. Since the amount of fine-tuning is determined almost completely by the masses of the top squarks, this could help a lot unless there is some other requirement that bounds the top squark masses from below. This is the place where the condition (iii) comes in — given the direct search bound of $m_{\tilde{e}} \gtrsim 100$ GeV, naturalness requires that either the top quark and Higgs boson are both rather heavy, $m_t \simeq (180 \sim 182)$ GeV and $M_{\text{Higgs}} \simeq (200 \sim 250)$ GeV, or that we have to break the unified mass relation to make the top squarks sufficiently light to evade fine-tuning. In this paper we have focused on the latter.

The low mediation scale, together with the absence of supersymmetric flavor changing neutral currents, suggests that supersymmetry breaking is mediated from the dynamical supersymmetry breaking (DSB) sector to the visible sector through standard model gauge interactions. The simplest theories of this kind arise if the DSB sector is charged under the standard model gauge group so that the superparticle masses are automatically generated once supersymmetry is broken in this sector. Since the DSB sector is charged under the standard model gauge group, it contributes to the evolution of the $SU(3)_C \times SU(2)_L \times U(1)_Y$ (321) gauge couplings. The successful supersymmetric prediction for gauge coupling unification is then preserved if this sector possesses an approximate global $SU(5)$ symmetry above M_{mess} , which contains the 321 gauge group as a subgroup. In fact, this becomes almost the necessary requirement if we want to formulate this class of theories using the “dual” description in higher dimensional warped spacetime, because the DSB sector is then strongly coupled over a wide energy interval above M_{mess} and the contribution to the evolution of the 321 gauge couplings is controlled only by imposing the global $SU(5)$ symmetry to this sector.

The presence of the global $SU(5)$ symmetry above M_{mess} and the absence of the unified mass relations for the squarks and sleptons implies that $SU(5)$ is broken dynamically to the 321 subgroup at the scale M_{mess} . This leads to light scalar states in the DSB sector, *xyons*, which are the pseudo-Goldstone bosons of this symmetry breaking. In the minimal case of the $SU(5)$ DSB sector, the 321 quantum numbers of xyons are given by $(\mathbf{3}, \mathbf{2})_{-5/6}$. We have estimated the mass of xyons in generic cases and calculated it in a class of calculable theories formulated in higher dimensions. We have found that the mass squared of xyons is positive in most of the parameter region, implying that the dynamical breaking of $SU(5)$ tends to align with the explicit breaking given by the gauging of the 321 subgroup. We have also found that the xyon mass is naturally in the multi-TeV region, $\approx (1 \sim 5)$ TeV, assuming that the DSB sector obeys naive dimensional analysis. In fact, it is natural to expect that the sizes of the operators in the DSB sector are determined by naive dimensional analysis; otherwise, incalculable threshold corrections to the 321 gauge couplings at M_{mess} would likely destroy the successful prediction associated with gauge coupling unification.

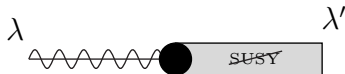


Figure 6: The diagram giving Dirac masses for the gauginos, where λ' represents the Dirac partners of the MSSM gaugino states, λ .

We emphasize that our argument is quite general and relies only on the assumption that the squark and slepton masses are generated through standard model gauge interactions. In particular, it is independent of the physics providing the extra Higgs quartic couplings, the sector that has a large model dependence. Our framework is also independent of the way the gauginos obtain masses. For instance, the gauginos can obtain Dirac masses through the diagrams of Fig. 6 if the DSB sector provides the Dirac partners of the MSSM gaugino states. The masses of the gauginos are then given by

$$M_i \simeq g_i \frac{\hat{b}^{1/2}}{4\pi} (\hat{\zeta}_i M_\rho), \quad (52)$$

in which case the ratios of the gaugino masses to the squark and slepton masses are significantly larger than in the Majorana case of Eq. (8). It is also possible that some of the 321 gauginos are Majorana fermions while the others are Dirac or pseudo-Dirac fermions. The point is that, even in these cases, the diagrams giving the squark and slepton masses are still those of Fig. 1b, so that the squark and slepton masses are given by the expressions in Eq. (9). Therefore, to avoid the unwanted unified mass relations of Eq. (3) we still need to break $SU(5)$ at the scale M_{mess} (we need to break $\hat{\zeta}_1 = \hat{\zeta}_2 = \hat{\zeta}_3$). The values for the xyon mass are not much affected either, because in the 4D picture the xyon mass arises from the diagrams with one loop of the 321 gauge multiplets, whose sizes do not depend much on the structure of the gaugino masses.

In fact, the class of theories discussed above can be constructed in a simple way as follows. In our warped spacetime with the bulk $SU(5)$ gauge group reduced to 321 both on the UV and the IR branes, we can introduce an extra $U(1)$ gauge field together with three chiral superfields $A_3(\mathbf{8}, \mathbf{1})_0$, $A_2(\mathbf{1}, \mathbf{3})_0$ and $A_1(\mathbf{1}, \mathbf{1})_0$ on the IR brane. We then break the extra $U(1)$ via the Higgs mechanism. Specifically, we introduce a pair of chiral superfields Φ and $\bar{\Phi}$ on the IR brane, which have $U(1)$ charges of $+1$ and -1 , respectively, and have different supersymmetry-breaking masses, $m_\Phi^2 \neq m_{\bar{\Phi}}^2$, through different couplings to the supersymmetry-breaking field, $\mathcal{L} \sim 2\delta(y - \pi R) \int d^4\theta (\kappa Z^\dagger Z \Phi^\dagger \Phi + \bar{\kappa} Z^\dagger Z \bar{\Phi}^\dagger \bar{\Phi})$ with $\kappa \neq \bar{\kappa}$. Assuming that m_Φ^2 and $m_{\bar{\Phi}}^2$ satisfy $m_\Phi^2 m_{\bar{\Phi}}^2 < 0$ and $m_\Phi^2 + m_{\bar{\Phi}}^2 > 0$, we have a stable vacuum in which a non-vanishing D -term for the $U(1)$ is generated. This D -term then gives Dirac masses for the gauginos through the operators

$\mathcal{L} \sim 2\delta(y - \pi R)\{\int d^2\theta \sum_{i=1,2,3} \mathcal{W}'^\alpha \mathcal{W}_{i\alpha} A_i + \text{h.c.}\}$, where \mathcal{W}'_α is the field-strength superfield for the extra $U(1)$ [53].²⁵ This model is similar to that discussed in [54]. The main difference, however, is that here we work in the context of [3] so that $SU(5)$ is broken on the IR brane and the coefficients of the above gaugino mass operators do not respect $SU(5)$. This is required to break the unwanted unified mass relations for the squarks and sleptons, and thus to eliminate the fine-tuning. Another interesting feature of the present model is that the gauginos can be purely Dirac fermions, which contrasts with the case in [54] where the gauginos can only be pseudo-Dirac fermions due to an unbroken $SU(5)$ on the IR brane. This provides a rather simple solution to the supersymmetric CP problem; with the minimal two Higgs-doublet structure for the Higgs sector, all the complex phases can be absorbed into the phases of the fields by the usual R and Peccei-Quinn rotations and the chiral rotations for the Dirac gaugino fields.

We can also go further in the Higgs sector. The point here is that physics on the IR brane does not affect physics above M_{mess} , so that we can do whatever we want on the IR brane without destroying the successes of supersymmetric theories — we can introduce arbitrary 321 multiplets with arbitrary couplings on the IR brane. For example, we can introduce an additional pair of Higgs doublets together with a singlet field on the IR brane to push the mass of the physical Higgs boson up to about 250 GeV [13] and/or modify the Higgs potential by introducing an IR-brane superpotential coupling(s) of the form $T_{-1}H_D H_D$, $T_{+1}\bar{H}_D \bar{H}_D$ or $T_0 H_D \bar{H}_D$, where T_Y represents an $SU(2)_L$ -triplet superfield with the hypercharge Y . In fact, this large freedom for physics on the IR brane, which is equivalent to the freedom for the IR dynamics of the DSB sector, opens up a very large class of model building possibilities for supersymmetric theories without fine-tuning, in the framework discussed in this paper.

In any of the theories described above, xions are naturally expected to be in the multi-TeV region. We have studied in detail the experimental signatures of these particles at the LHC and at the VLHC. We have found that a generic signature is highly ionizing tracks caused by stable charged bound states of xions: the lightest charged xymeson \tilde{T}^- . We have found that the reach of the LHC in the xion mass is about $(2.0 \sim 2.2)$ TeV, so that xions may be discovered at the LHC. At the VLHC, the reach in the xion mass is about 5.0 TeV (13 TeV) for a center-of-mass energy of 50 TeV (200 TeV). In the holographic 5D theories, this covers the entire parameter region for the IR-brane scale of $k' \lesssim 13$ TeV (33 TeV). Since we naturally expect $k' \approx 10$ TeV to obtain weak-scale superparticle masses, the discovery of xions at the VLHC is quite promising.

²⁵We assume that the tree-level kinetic mixing between the extra $U(1)$ and hypercharge is suppressed. Potentially dangerous effects of introducing the singlet field A_1 can also be suppressed, for example, if Z is charged under an R symmetry and the theory possesses an approximate symmetry $A_1 \rightarrow -A_1$ (i.e. the coefficients of the operators containing the odd number of A_1 are somewhat suppressed, say by an order of magnitude). This leads to a scenario in which the Dirac bino is significantly lighter than the other gauginos and the right-handed selectron masses are generated mainly by the D -term VEV of $U(1)_Y$.

We have also discussed cosmology in our scenario. We have found that if the stable lightest xymeson is neutral and there is strong nonperturbative xyon annihilation at the QCD era, the thermal history of the universe can be standard. Alternatively, the xyon lifetime may be shorter than about 100 sec, in which case the thermal history may also be standard even without nonperturbative annihilation. In these cases, dark matter can naturally arise as thermal relic particles. In particular, we have considered a class of dark matter, which arises as a composite state of the DSB sector but interacts with the MSSM states through mixings between the elementary states and the composite DSB states. The correct dark matter abundance is naturally reproduced, but direct detection will be difficult because the characteristic mass scale for this dark matter is of order $(10 \sim 100)$ TeV, rather than the conventional one of order $(0.1 \sim 1)$ TeV. A consistent cosmological scenario can be obtained, since the theories do not have any dangerous relics and the reheating temperature after inflation can be high. In particular, the gravitino does not cause any cosmological problem as it is very light with $m_{3/2} \simeq (0.1 \sim 10)$ eV.

We find it is quite encouraging that we have obtained a consistent picture of supersymmetric theories that do not suffer from fine-tuning in electroweak symmetry breaking. A thorough study of the parameter space of the class of theories discussed here is warranted. Much model building work will also be possible in the present framework. In particular, detailed exploration of the Higgs sector will be one of the important issues.

Acknowledgments

This work was supported in part by the Director, Office of Science, Office of High Energy and Nuclear Physics, of the US Department of Energy under Contract DE-AC03-76SF00098 and DE-FG03-91ER-40676. The work of Y.N. was also supported by the National Science Foundation under grant PHY-0403380 and by a DOE Outstanding Junior Investigator award.

Appendix A

In this Appendix we present the calculations of the xyon mass in the holographic higher dimensional theories discussed in section 4.2. We also present, for completeness, the expressions for the masses of the MSSM superparticles and the superpartners of xyons.

A.1 Lagrangian of the gauge sector

The Lagrangian of the gauge sector of the theory is given by [3]

$$S = \int d^4x \int_0^{\pi R} dy \left\{ \mathcal{L}_{\text{bulk}} + 2\delta(y)\mathcal{L}_{\text{UV}} + 2\delta(y - \pi R)\mathcal{L}_{\text{IR}} \right\}, \quad (53)$$

where

$$\mathcal{L}_{\text{bulk}} = \left\{ \frac{1}{4\kappa g_5^2} \int d^2\theta \text{Tr}[\mathcal{W}^\alpha \mathcal{W}_\alpha] + \text{h.c.} \right\} + \frac{e^{-2k|y|}}{4\kappa g_5^2} \int d^4\theta \text{Tr}[\mathcal{A}^2], \quad (54)$$

$$\mathcal{L}_{\text{UV}} = \sum_{i=1,2,3} \left\{ \frac{1}{4\kappa \tilde{g}_{0,i}^2} \int d^2\theta \text{Tr}[\mathcal{W}_i^\alpha \mathcal{W}_{i\alpha}] + \text{h.c.} \right\}, \quad (55)$$

$$\begin{aligned} \mathcal{L}_{\text{IR}} = & \sum_{i=1,2,3} \left\{ - \int d^2\theta \frac{\zeta_i}{2\kappa M_*} Z \text{Tr}[\mathcal{W}_i^\alpha \mathcal{W}_{i\alpha}] + \text{h.c.} \right\} \\ & + e^{-2\pi k R} \int d^4\theta \left(\frac{\eta}{4\kappa M_*} Z^\dagger + \frac{\eta^*}{4\kappa M_*} Z - \frac{\rho}{8\kappa M_*^2} Z^\dagger Z \right) \text{Tr}[\mathcal{P}[\mathcal{A}]\mathcal{P}[\mathcal{A}]], \end{aligned} \quad (56)$$

and

$$\mathcal{A} \equiv e^{-2V}(\partial_y e^{2V}) - \sqrt{2} e^{-2V} \Sigma^\dagger e^{2V} - \sqrt{2} \Sigma, \quad (57)$$

(here we have neglected unimportant IR-brane localized gauge kinetic terms). The trace is over the $SU(5)$ space and $\mathcal{P}[\mathcal{X}]$ is a projection operator: with \mathcal{X} an adjoint of $SU(5)$, $\mathcal{P}[\mathcal{X}]$ extracts the $(\mathbf{3}, \mathbf{2})_{-5/6} + (\mathbf{3}^*, \mathbf{2})_{5/6}$ component of \mathcal{X} under the decomposition to 321. The $SU(5)$ field-strength superfield is defined by $\mathcal{W}_\alpha \equiv -(1/8)\bar{D}^2(e^{-2V}\mathcal{D}_\alpha e^{2V})$, and $\mathcal{W}_{i\alpha}$ with $i = 1, 2, 3$ are the field-strength superfields for the $U(1)_Y$, $SU(2)_L$ and $SU(3)_C$ subgroups ($\mathcal{W}_{i\alpha} \subset \mathcal{W}_\alpha$). The normalization for the $SU(5)$ generators is given by $\text{Tr}[T^A T^B] = \kappa \delta^{AB}$ where $A, B = 1, \dots, 24$.

The Lagrangian in components is obtained by expanding Eqs. (54 – 56) in component fields:

$$V = -\theta^\alpha \sigma_{\alpha\dot{\alpha}}^\mu \bar{\theta}^{\dot{\alpha}} A_\mu - i e^{-\frac{3}{2}k|y|} \bar{\theta}^2 \theta^\alpha \lambda_\alpha + i e^{-\frac{3}{2}k|y|} \theta^2 \bar{\theta}_{\dot{\alpha}} \lambda^{\dot{\alpha}} + \frac{1}{2} e^{-2k|y|} \theta^2 \bar{\theta}^2 D, \quad (58)$$

$$\Sigma = \frac{1}{\sqrt{2}}(\chi + iA_5) - \sqrt{2} i e^{-\frac{1}{2}k|y|} \theta^\alpha \lambda'_\alpha + e^{-k|y|} \theta^2 F_\Sigma, \quad (59)$$

where $A_\mu = A_\mu^A T^A$, $A_5 = A_5^A T^A$, $\lambda_\alpha = \lambda_\alpha^A T^A$, $\lambda'_\alpha = \lambda'_\alpha^A T^A$, $\chi = \chi^A T^A$, $D = D^A T^A$, and $F_\Sigma = F_\Sigma^A T^A$. The result is again written in the form of Eq. (53) with

$$\mathcal{L}_{\text{bulk}} = \frac{1}{g_5^2} \left[-\frac{1}{4} F^{\mu\nu A} F_{\mu\nu}^A - \frac{1}{2} e^{-2k|y|} F^{\mu 5 A} F_{\mu 5}^A - \frac{1}{2\xi} \left\{ (\partial^\mu A_\mu^A) + \xi \partial^y (e^{-2k|y|} A_5^A) \right\}^2 \right]$$

$$\begin{aligned}
& -\frac{1}{2}e^{-2k|y|}(\mathcal{D}^\mu\chi^A)(\mathcal{D}_\mu\chi^A) - ie^{-3k|y|}(\lambda_{\dot{\alpha}}^{\dagger A}\bar{\sigma}^{\mu\dot{\alpha}\alpha}\overleftrightarrow{\mathcal{D}}_\mu\lambda_\alpha^A) - ie^{-3k|y|}(\lambda_{\dot{\alpha}}^{\dagger A}\bar{\sigma}^{\mu\dot{\alpha}\alpha}\overleftrightarrow{\mathcal{D}}_\mu\lambda_\alpha^{\prime A}) \\
& - e^{-4k|y|}(\lambda^{\prime\alpha A}\overleftrightarrow{\mathcal{D}}_y\lambda_\alpha^A) - e^{-4k|y|}(\lambda_{\dot{\alpha}}^{\dagger A}\overleftrightarrow{\mathcal{D}}_y\lambda^{\dagger\dot{\alpha}A}) - \frac{k}{2}\epsilon(y)e^{-4k|y|}(\lambda^{\alpha A}\lambda_\alpha^{\prime A} + \lambda_{\dot{\alpha}}^{\dagger A}\lambda^{\dagger\dot{\alpha}A}) \\
& + \frac{1}{2}e^{-4k|y|}D^AD^A + e^{-4k|y|}F_\Sigma^{\dagger A}F_\Sigma^A + e^{-4k|y|}(D^A\overleftrightarrow{\mathcal{D}}_y\chi^A) \\
& + ie^{-4k|y|}f^{ABC}\lambda^{\prime\alpha A}\chi^B\lambda_\alpha^C - ie^{-4k|y|}f^{ABC}\lambda_{\dot{\alpha}}^{\dagger A}\chi^B\lambda^{\dagger\dot{\alpha}C}], \tag{60}
\end{aligned}$$

$$\mathcal{L}_{\text{UV}} = \sum_{i=1,2,3} \frac{1}{\tilde{g}_{0,i}^2} \left\{ -\frac{1}{4}F_i^{\mu\nu a}F_{i\mu\nu}^a - i(\lambda_{i\dot{\alpha}}^{\dagger a}\bar{\sigma}^{\mu\dot{\alpha}\alpha}\overleftrightarrow{\mathcal{D}}_\mu\lambda_{i\alpha}^a) + \frac{1}{2}D_i^aD_i^a \right\}, \tag{61}$$

$$\begin{aligned}
\mathcal{L}_{\text{IR}} = \sum_{i=1,2,3} & \left\{ -\frac{1}{2}\frac{\zeta_i F_Z}{M_*}e^{-4\pi kR}\lambda_i^{\alpha a}\lambda_{i\alpha}^a - \frac{1}{2}\frac{\zeta_i^* F_Z^*}{M_*}e^{-4\pi kR}\lambda_{i\dot{\alpha}}^{\dagger a}\lambda_i^{\dagger\dot{\alpha}a} \right\} \\
& - \frac{1}{2}\frac{\eta F_Z^*}{M_*}e^{-4\pi kR}\lambda^{\prime\alpha\hat{a}}\lambda_\alpha^{\hat{a}} - \frac{1}{2}\frac{\eta^* F_Z}{M_*}e^{-4\pi kR}\lambda_{\dot{\alpha}}^{\dagger\hat{a}}\lambda^{\dagger\dot{\alpha}\hat{a}} \\
& - \sqrt{2}\frac{\eta F_Z^*}{M_*}e^{-4\pi kR}\chi^{\hat{a}}F_\Sigma^{\hat{a}} - \sqrt{2}\frac{\eta^* F_Z}{M_*}e^{-4\pi kR}\chi^{\hat{a}}F_\Sigma^{\dagger\hat{a}} - \frac{1}{2}\frac{\rho|F_Z|^2}{M_*^2}e^{-4\pi kR}\chi^{\hat{a}}\chi^{\hat{a}}, \tag{62}
\end{aligned}$$

where F_Z is defined by $\langle Z \rangle = -e^{-\pi kR}F_Z\theta^2$, and the indices a and \hat{a} run over the 321 and XY components, respectively: $A = \{a, \hat{a}\}$ (summation convention implied for A , a and \hat{a}). The function $\epsilon(y)$ takes $+1$ for $y > 0$ and -1 for $y < 0$, \mathcal{D}_μ and \mathcal{D}_y are the gauge covariant derivatives, and $\overleftrightarrow{\mathcal{D}}_\mu$ and $\overleftrightarrow{\mathcal{D}}_y$ are defined by $(\varphi_1\overleftrightarrow{\mathcal{D}}_M\varphi_2) \equiv (1/2)\{\varphi_1(\mathcal{D}_M\varphi_2) - (\mathcal{D}_M\varphi_1)\varphi_2\}$ for arbitrary fields φ_1 and φ_2 , where $M = \mu, y$. Here, we have added the gauge-fixing term

$$S_{\text{GF}} = \int d^4x \int_0^{\pi R} dy \frac{1}{g_5^2} \left[-\frac{e^{-4k|y|}}{2\xi} \left\{ e^{2k|y|}(\partial^\mu A_\mu^A) + \xi e^{2k|y|}\partial^y(e^{-2k|y|}A_5^A) \right\}^2 \right], \tag{63}$$

in the original Lagrangian to obtain Eqs. (60 – 62).

A.2 Superparticle masses

The masses of the gauginos and their KK towers are obtained by solving the equations of motion derived from Eqs. (60 – 62). The equation determining these masses, m_n , are given by [32]

$$\frac{J_0\left(\frac{m_n}{k}\right) + \frac{g_5^2}{\tilde{g}_{0,i}^2}m_n J_1\left(\frac{m_n}{k}\right)}{Y_0\left(\frac{m_n}{k}\right) + \frac{g_5^2}{\tilde{g}_{0,i}^2}m_n Y_1\left(\frac{m_n}{k}\right)} = \frac{J_0\left(\frac{m_n}{k'}\right) + g_5^2 M_{\lambda,i} J_1\left(\frac{m_n}{k'}\right)}{Y_0\left(\frac{m_n}{k'}\right) + g_5^2 M_{\lambda,i} Y_1\left(\frac{m_n}{k'}\right)}, \tag{64}$$

where $M_{\lambda,i} \equiv \zeta_i F_Z/M_*$ (see Eq. (24)). For $m_n/k' \ll 1$ and $g_5^2 m_n M_{\lambda,i}/k' \ll 1$, which are satisfied for the lowest modes if the sizes of various parameters are determined by naive dimensional analysis ($r_{\lambda,i} \sim 1$; see Eq. (25)), the 321 gaugino masses are given by $m_{\lambda_i^{321}} \simeq g_i^2 M_{\lambda,i} e^{-\pi kR}$, in agreement with Eq. (30) obtained by 4D considerations. Here, $g_i = (\pi R/g_5^2 + 1/\tilde{g}_{0,i}^2)^{-1/2}$ are the

4D gauge couplings. The squark and slepton masses are generated at one loop and given by

$$m_{\tilde{f}}^2 = \frac{1}{2\pi^2} \sum_{i=1,2,3} C_i^{\tilde{f}} \int_0^\infty dq q^3 \left\{ f^{321,i}(1/k, 1/k; q) - f^{321,i}(1/k, 1/k; q) \Big|_{M_{\lambda,i}=0} \right\}, \quad (65)$$

where $\tilde{f} = \tilde{q}, \tilde{u}, \tilde{d}, \tilde{l}, \tilde{e}$ represents the MSSM squarks and sleptons, and the $C_i^{\tilde{f}}$ are the group theoretical factors given by $(C_1^{\tilde{f}}, C_2^{\tilde{f}}, C_3^{\tilde{f}}) = (1/60, 3/4, 4/3), (4/15, 0, 4/3), (1/15, 0, 4/3), (3/20, 3/4, 0)$ and $(3/5, 0, 0)$ for $\tilde{f} = \tilde{q}, \tilde{u}, \tilde{d}, \tilde{l}$ and \tilde{e} , respectively. The functions $f^{321,i}(z, z'; q)$ arise from the 321 gaugino propagators whose explicit form are given in Appendix B.1 (see Eqs. (88, 92, 93)).

The masses for the superpartners of xyons, λ^{XY} and χ^{XY} , are given as the lowest solutions of

$$\frac{J_1\left(\frac{m_n}{k}\right)}{Y_1\left(\frac{m_n}{k}\right)} = \frac{J_1\left(\frac{m_n}{k'}\right) - g_5^2 M_{\lambda,X} J_0\left(\frac{m_n}{k'}\right)}{Y_1\left(\frac{m_n}{k'}\right) - g_5^2 M_{\lambda,X} Y_0\left(\frac{m_n}{k'}\right)}, \quad (66)$$

and

$$\frac{J_1\left(\frac{m_n}{k}\right)}{Y_1\left(\frac{m_n}{k}\right)} = \frac{J_1\left(\frac{m_n}{k'}\right) - \frac{g_5^2 M_{\chi,X}^2 k'}{m_n k} J_0\left(\frac{m_n}{k'}\right)}{Y_1\left(\frac{m_n}{k'}\right) - \frac{g_5^2 M_{\chi,X}^2 k'}{m_n k} Y_0\left(\frac{m_n}{k'}\right)}, \quad (67)$$

respectively [3]. Here, $M_{\lambda,X} \equiv \eta F_Z^*/M_*$, $M_{\chi,X}^2 \equiv \rho' |F_Z|^2/M_*^2$ (see Eq. (24)), and $\rho' \equiv \rho + 8g_5^2 |\eta|^2 \delta(0)$ (see Eq. (23)). For natural sizes of the couplings, suggested by naive dimensional analysis, these masses are of order $\pi k'$.

A.3 Xyon mass

To calculate the mass of xyons, we need to know their wavefunctions. In our 5D theory, xyons correspond to the lowest modes for A_5^{XY} . The wavefunctions of these modes are obtained by solving the equations of motion for A_5^{XY} , given by the Lagrangian of Eq. (60). Writing xyon fields as $\varphi^{\hat{a}}(x)$, we find in the Feynman-'t Hooft gauge ($\xi = 1$)

$$A_5^{\hat{a}}(x, y) = \sqrt{\frac{2g_5^2 k}{e^{2\pi k R} - 1}} e^{2k|y|} \varphi^{\hat{a}}(x), \quad (68)$$

where $\varphi^{\hat{a}}(x)$ is canonically normalized in 4D.

The mass of xyons are calculated most easily using the on-shell Lagrangian, which is obtained from Eqs. (60 – 62) by integrating out the auxiliary fields:

$$S = \int d^4x \int_0^{\pi R} dy \left\{ \mathcal{L}_{\text{gauge}} + \mathcal{L}_{\text{gaugino}} + \mathcal{L}_{\text{scalar}} + \mathcal{L}_{\text{Yukawa}} \right\}. \quad (69)$$

Here,

$$\mathcal{L}_{\text{gauge}} = \frac{1}{g_5^2} \left[-\frac{1}{4} F^{\mu\nu A} F_{\mu\nu}^A - \frac{1}{2} e^{-2k|y|} F^{\mu 5 A} F_{\mu 5}^A - \frac{1}{2} \left\{ (\partial^\mu A_\mu^A) + \partial^y (e^{-2k|y|} A_5^A) \right\}^2 \right], \quad (70)$$

$$\begin{aligned}
\mathcal{L}_{\text{gaugino}} = & \frac{1}{g_5^2} \left[-ie^{-3k|y|} (\lambda_{\hat{\alpha}}^{\dagger A} \bar{\sigma}^{\mu\hat{\alpha}\alpha} \overleftrightarrow{\mathcal{D}}_{\mu} \lambda_{\alpha}^A) - ie^{-3k|y|} (\lambda_{\hat{\alpha}}^{\dagger A} \bar{\sigma}^{\mu\hat{\alpha}\alpha} \overleftrightarrow{\mathcal{D}}_{\mu} \lambda_{\alpha}^{\prime A}) \right. \\
& \left. - e^{-4k|y|} (\lambda^{\prime\alpha A} \overleftrightarrow{\mathcal{D}}_y \lambda_{\alpha}^A) - e^{-4k|y|} (\lambda_{\hat{\alpha}}^{\prime\dagger A} \overleftrightarrow{\mathcal{D}}_y \lambda^{\dagger\hat{\alpha}A}) - \frac{k}{2} \epsilon(y) e^{-4k|y|} (\lambda^{\alpha A} \lambda_{\alpha}^{\prime A} + \lambda_{\hat{\alpha}}^{\dagger A} \lambda^{\dagger\hat{\alpha}A}) \right] \\
& + 2\delta(y - \pi R) \left[\sum_{i=1,2,3} \left\{ -\frac{1}{2} e^{-4\pi k R} M_{\lambda,i} \lambda_i^{\alpha\alpha} \lambda_{i\alpha}^a - \frac{1}{2} e^{-4\pi k R} M_{\lambda,i}^* \lambda_{i\hat{\alpha}}^{\dagger a} \lambda_i^{\dagger\hat{\alpha}a} \right\} \right. \\
& \left. - \frac{1}{2} e^{-4\pi k R} M_{\lambda,X} \lambda^{\prime\alpha\hat{a}} \lambda_{\alpha}^{\hat{a}} - \frac{1}{2} e^{-4\pi k R} M_{\lambda,X}^* \lambda_{\hat{\alpha}}^{\prime\dagger\hat{a}} \lambda^{\dagger\hat{\alpha}\hat{a}} \right], \tag{71}
\end{aligned}$$

$$\begin{aligned}
\mathcal{L}_{\text{scalar}} = & \frac{1}{g_5^2} \left[-\frac{1}{2} e^{-2k|y|} (\mathcal{D}^{\mu} \chi^A) (\mathcal{D}_{\mu} \chi^A) - \frac{1}{2} e^{-4k|y|} (\mathcal{D}^y \chi^A) (\mathcal{D}_y \chi^A) \right. \\
& \left. + 2k^2 e^{-4k|y|} \chi^A \chi^A - 2k e^{-4k|y|} \{ \delta(y) - \delta(y - \pi R) \} \chi^A \chi^A \right] \\
& + 2\delta(y - \pi R) \left[-\frac{1}{2} e^{-4\pi k R} M_{\chi,X}^2 \chi^{\hat{a}} \chi^{\hat{a}} \right], \tag{72}
\end{aligned}$$

$$\mathcal{L}_{\text{Yukawa}} = \frac{1}{g_5^2} \left[ie^{-4k|y|} f^{ABC} \lambda^{\prime\alpha A} \chi^B \lambda_{\alpha}^C - ie^{-4k|y|} f^{ABC} \lambda_{\hat{\alpha}}^{\prime\dagger A} \chi^B \lambda^{\dagger\hat{\alpha}C} \right], \tag{73}$$

where $M_{\lambda,i} = \zeta_i F_Z / M_*$, $M_{\lambda,X} = \eta F_Z^* / M_*$, $M_{\chi,X}^2 = \rho^2 |F_Z|^2 / M_*^2$, and we have taken the Feynman-'t Hooft gauge, $\xi = 1$. We have also suppressed the contributions from the UV-brane localized gauge kinetic terms, for the simplicity of the presentation.

From Eqs. (69 – 73), we find that at one loop the xyon mass receives contributions from the diagrams with $A_{\mu}^{321} - A_5^{XY}$, $A_{\mu}^{XY} - A_5^{321}$, $A_{\mu}^{321} - A_{\mu}^{XY}$, $\lambda^{321} - \lambda^{\prime XY}$, $\lambda^{XY} - \lambda^{\prime 321}$ and $\chi^{321} - \chi^{\prime XY}$ loops using two 3-point vertices, and from the diagrams with A_{μ}^{321} , A_{μ}^{XY} , χ^{321} and $\chi^{\prime XY}$ loops using one 4-point vertex (and the ghost loops). Instead of calculating all these loops, here we use the following trick to simplify the calculation of the xyon mass. We use the fact that the xyon mass is not generated in the supersymmetric limit. The xyon mass, then, can be obtained by calculating the diagrams that contain the effects of supersymmetry breaking and subtracting the values of the same diagrams in the supersymmetric limit. In this procedure, we have to calculate only the diagrams given in Fig. 7. We then obtain the xyon mass by subtracting the values of the same diagrams with $M_{\lambda,i}$, $M_{\lambda,X}$ and $M_{\chi,X}^2$ set to zero.

We start by the gaugino-loop diagrams of Fig. 7a and 7b. We first note that the gaugino mass parameters on the IR brane are, in general, arbitrary complex parameters. We take this into account by rewriting $M_{\lambda,i} \rightarrow M_{\lambda,i} e^{i\phi_i}$ and $M_{\lambda,X} \rightarrow M_{\lambda,X} e^{i\phi_X}$, so $M_{\lambda,i}$ and $M_{\lambda,X}$ are now real parameters. Calculating the diagrams in Fig. 7a and 7b, we obtain the following contribution to the xyon mass:

$$\delta \hat{m}_{\varphi}^2|_{\lambda} = \delta \hat{m}_{\varphi}^2|_{\lambda}^{(1)} + \sum_{i=1,2,3} \cos(\phi_i + \phi_X) \delta \hat{m}_{\varphi}^2|_{\lambda,i}^{(2)}. \tag{74}$$

Here, the first term in the right-hand-side is the piece that does not depend on the phases of the

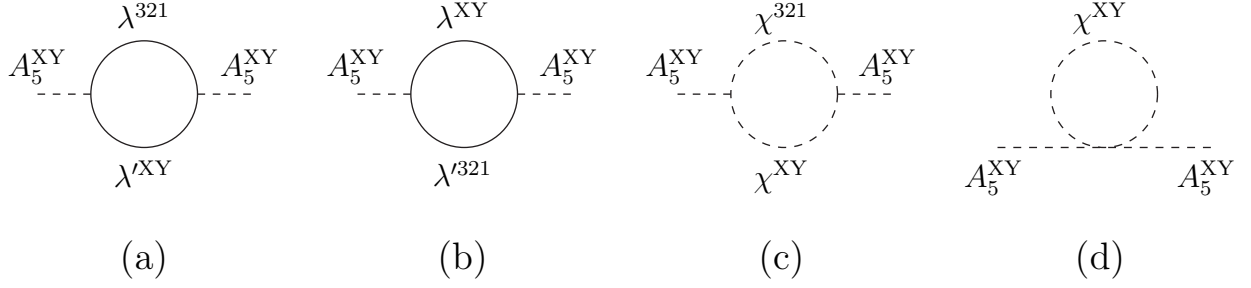


Figure 7: One-loop diagrams relevant for the calculation of the xyon mass.

gaugino mass parameters:

$$\delta\hat{m}_\varphi^2|_\lambda^{(1)} = \delta m_\varphi^2|_\lambda^{(1)} - \delta m_\varphi^2|_{\lambda, M_\lambda, i=M_\lambda, X=0}^{(1)}, \quad (75)$$

where

$$\begin{aligned} \delta m_\varphi^2|_\lambda^{(1)} &= -\frac{1}{2\pi^2} \sum_{i=1,2,3} \frac{C_i^\varphi}{(g_5^2 k)^2} \int \frac{dz_1 dz_2}{z_1 z_2} \mathcal{F}(z_1) \mathcal{F}(z_2) \int d|p| |p|^3 \\ &\times \left[|p|^2 f'^{321,i}(z_2, z_1; p) f'^{XY}(z_1, z_2; p) + |p|^2 f'^{XY}(z_2, z_1; p) f'^{321,i}(z_1, z_2; p) \right. \\ &\left. + 2 \left\{ \left(\partial_{z_2} - \frac{1}{2z_2} \right) f'^{321,i}(z_2, z_1; p) \right\} \left\{ \left(\partial_{z_1} - \frac{1}{2z_1} \right) f'^{XY}(z_1, z_2; p) \right\} \right]. \quad (76) \end{aligned}$$

We here subtracted the supersymmetric piece in Eq. (75). The functions $f^{321,i}$, f^{XY} , $f'^{321,i}$ and f'^{XY} are given in Appendix B.1. The function $\mathcal{F}(z)$ is the wavefunction of xyons in the z coordinate

$$\mathcal{F}(z) = \sqrt{\frac{2g_5^2 k}{e^{2\pi k R} - 1}} (kz)^2, \quad (77)$$

(see Eq. (68)), and C_i^φ are the group theoretical factors: $(C_1^\varphi, C_2^\varphi, C_3^\varphi) = (5/12, 3/4, 4/3)$ for $SU(5)$ xyons. The second term in the right-hand-side of Eq. (74) is the piece that depends on the phases:

$$\delta\hat{m}_\varphi^2|_{\lambda,i}^{(2)} = \delta m_\varphi^2|_{\lambda,i}^{(2)} - \delta m_\varphi^2|_{\lambda,i, M_\lambda, i=M_\lambda, X=0}^{(2)}, \quad (78)$$

where

$$\begin{aligned} \delta m_\varphi^2|_{\lambda,i}^{(2)} &= \frac{1}{2\pi^2} \frac{C_i^\varphi}{(g_5^2 k)^2} \int \frac{dz_1 dz_2}{z_1 z_2} \mathcal{F}(z_1) \mathcal{F}(z_2) \int d|p| |p|^3 \\ &\times \left[h'^{321,i}(z_2, z_1; p) h'^{XY}(z_1, z_2; p) + h'^{XY}(z_2, z_1; p) h'^{321,i}(z_1, z_2; p) \right. \\ &\left. + \frac{2}{|p|^2} \left\{ \left(\partial_{z_2} - \frac{1}{2z_2} \right) h'^{321,i}(z_2, z_1; p) \right\} \left\{ \left(\partial_{z_1} - \frac{1}{2z_1} \right) h'^{XY}(z_1, z_2; p) \right\} \right]. \quad (79) \end{aligned}$$

The functions $h^{321,i}$, h^{XY} , $h'^{321,i}$ and h'^{XY} are given in Appendix B.1.

We next consider the contributions from gauge-scalar loops. They are given by

$$\delta\hat{m}_\varphi^2|_\chi = \delta\hat{m}_\varphi^2|_\chi^{(1)} + \delta\hat{m}_\varphi^2|_\chi^{(2)}. \quad (80)$$

The first term in the right-hand-side represents the contribution from the diagram of Fig. 7c:

$$\delta\hat{m}_\varphi^2|_\chi^{(1)} = \delta m_\varphi^2|_\chi^{(1)} - \delta m_\varphi^2|_{\chi, M_{\chi,X}^2=0}^{(1)}, \quad (81)$$

where

$$\begin{aligned} \delta m_\varphi^2|_\chi^{(1)} &= \frac{C^\varphi}{8\pi^2 g_5^4} \int dz_1 dz_2 \mathcal{F}(z_1) \mathcal{F}(z_2) \int d|p| |p|^3 \\ &\times \left[\partial_{z_1} \partial_{z_2} \left(\hat{G}_{\chi\chi}^{321}(z_1, z_2; p) \hat{G}_{\chi\chi}^{XY}(z_1, z_2; p) \right) - 4 \left(\partial_{z_1} \hat{G}_{\chi\chi}^{321}(z_1, z_2; p) \right) \left(\partial_{z_2} \hat{G}_{\chi\chi}^{XY}(z_1, z_2; p) \right) \right]. \end{aligned} \quad (82)$$

Here, $C^\varphi \equiv \sum_{i=1,2,3} C_i^\varphi = 5/2$, and $\hat{G}_{\chi\chi}^{321}(z, z'; p)$ and $\hat{G}_{\chi\chi}^{XY}(z, z'; p)$ are the propagators for the (rescaled) gauge scalars, whose explicit forms are given in Appendix B.2. The second term in the right-hand-side of Eq. (80) is the contribution from the diagram of Fig. 7d:

$$\delta\hat{m}_\varphi^2|_\chi^{(2)} = \delta m_\varphi^2|_\chi^{(2)} - \delta m_\varphi^2|_{\chi, M_{\chi,X}^2=0}^{(2)}, \quad (83)$$

where

$$\delta m_\varphi^2|_\chi^{(2)} = \frac{iC^\varphi}{8\pi^2 (g_5^2 k)} \int \frac{dz}{z} \{ \mathcal{F}(z) \}^2 \int d|p| |p|^3 \hat{G}_{\chi\chi}^{XY}(z, z; p). \quad (84)$$

Here we note that the 4D-momentum integral in $\delta\hat{m}_\varphi^2|_\chi^{(2)}$ are divergent even after subtracting the supersymmetric piece. This contribution, however, is canceled by a part of the contribution arising from $\delta\hat{m}_\varphi^2|_\chi^{(1)}$ in the following way. In general, the propagators of 5D fields take the form of $\hat{G}(z, z'; p) = \theta(z - z') \mathcal{G}(z, z'; p) + \theta(z' - z) \mathcal{G}(z', z; p)$, where $\mathcal{G}(z, z'; p)$ is some function depending on the field of interest (this is implicit in the expressions of Appendix B, which use the symbols $z_<$ and $z_>$ instead of the theta function). This gives the contribution in Eq. (82) proportional to $\delta(z_1 - z_2)$ in the integrand, which arises from the piece with z -derivatives hitting the theta functions. We then find that the resulting contribution in $\delta\hat{m}_\varphi^2|_\chi^{(1)}$, which can be written in the form of a single z integral, is exactly canceled with $\delta\hat{m}_\varphi^2|_\chi^{(2)}$ in Eq. (80).

To summarize, the mass of xyons is given by

$$m_\varphi^2 = \delta\hat{m}_\varphi^2|_\lambda^{(1)} + \sum_{i=1,2,3} \cos(\phi_i + \phi_X) \delta\hat{m}_\varphi^2|_{\lambda,i}^{(2)} + \delta\hat{m}_\varphi^2|_\chi, \quad (85)$$

where $\delta\hat{m}_\varphi^2|_\lambda^{(1)}$, $\delta\hat{m}_\varphi^2|_{\lambda,i}^{(2)}$ and $\delta\hat{m}_\varphi^2|_\chi$ are given by Eqs. (75, 76), (78, 79) and (80 – 84), respectively. The quantities $\delta\hat{m}_\varphi^2|_\lambda^{(1)}$, $\delta\hat{m}_\varphi^2|_{\lambda,i}^{(2)}$ and $\delta\hat{m}_\varphi^2|_\chi$ are separately finite (up to exponentially suppressed

k'	$\frac{M_*}{\pi k}$	$\{r_{\lambda,1}, r_{\lambda,2}, r_{\lambda,3}, r_{\lambda,X}, r_{\chi,X}\}$	$[\{\delta\hat{m}_\varphi^2 _\lambda^{(1)}, \delta\hat{m}_\varphi^2 _{\lambda,1}^{(2)}, \delta\hat{m}_\varphi^2 _{\lambda,2}^{(2)}, \delta\hat{m}_\varphi^2 _{\lambda,3}^{(2)}, \delta\hat{m}_\varphi^2 _\chi\}]^{1/2}$					$[m_\varphi^2]^{1/2}$
10	3	1 1 1 1 1	3.7	0.04	0.1	0.3	-1.5	3.4
10	3	0.1 0.1 0.1 1 1	3.2	0.01	0.03	0.1	-1.5	2.9
10	3	1 1 1 0.1 1	2.0	0.04	0.1	0.3	-1.5	1.3
10	3	1 1 1 1 0.05	3.7	0.04	0.1	0.3	-1.0	3.6
10	3	0.1 0.1 0.1 0.1 1	0.8	0.01	0.03	0.1	-1.5	-1.3
10	3	2.5 0.9 1.0 1 1	3.7	0.05	0.1	0.3	-1.5	3.4
20	3	2.5 0.9 1.0 1 1	7.2	0.1	0.2	0.6	-3.0	6.5
40	3	2.5 0.9 1.0 1 1	14	0.2	0.4	1.2	-6.0	13
10	1	2.5 0.9 1.0 1 1	2.0	0.05	0.07	0.2	-1.2	1.7
10	10	2.5 0.9 1.0 1 1	5.1	0.03	0.08	0.2	-1.6	4.8

Table 1: Values of various contributions to the xyon mass squared for several sample parameter points. Here, $[X]^n \equiv \text{sgn}(X) \cdot |X|^n$, and all the masses are given in units of TeV.

contributions), reflecting the fact that the xyon obtains a mass only through the $SU(5)$ breaking on the UV brane while its wavefunction is strongly localized to the IR brane.

To see the relative importance of various contributions, we have listed values of $\delta\hat{m}_\varphi^2|_\lambda^{(1)}$, $\delta\hat{m}_\varphi^2|_{\lambda,i}^{(2)}$ and $\delta\hat{m}_\varphi^2|_\chi$ in Table 1 for several points in the parameter space. Here, $r_{\lambda,i}$, $r_{\lambda,X}$ and $r_{\chi,X}$ are dimensionless parameters defined by $r_{\lambda,i} = M_{\lambda,i}/(M_*/16\pi^2)$, $r_{\lambda,X} = M_{\lambda,X}/(M_*/16\pi^2)$ and $r_{\chi,X} = M_{\chi,X}^2/(M_*^2/16\pi^2)$, which naturally take values of order one (see Eq. (25)). From the table we find the following:

- The contributions to the xyon mass squared from the gaugino loop diagrams with the supersymmetric piece subtracted are positive, while that from the gauge-scalar loop diagrams with the supersymmetric piece subtracted is negative.
- In most of natural parameter regions, the xyon mass squared, m_φ^2 , is positive, which is crucial for the model to be viable.
- The sizes of phase-dependent gaugino contributions, $\delta\hat{m}_\varphi^2|_{\lambda,1}^{(2)}$, $\delta\hat{m}_\varphi^2|_{\lambda,2}^{(2)}$ and $\delta\hat{m}_\varphi^2|_{\lambda,3}^{(2)}$, are much smaller than that of the phase-independent one, $\delta\hat{m}_\varphi^2|_\lambda^{(1)}$. This implies that the size of the xyon mass does not depend much on the complex phases of the gaugino mass parameters on the IR brane.
- The values of $\delta\hat{m}_\varphi^2|_\lambda^{(1)}$, $\delta\hat{m}_\varphi^2|_{\lambda,1}^{(2)}$, $\delta\hat{m}_\varphi^2|_{\lambda,2}^{(2)}$ and $\delta\hat{m}_\varphi^2|_{\lambda,3}^{(2)}$ ($|\delta\hat{m}_\varphi^2|_\chi|$) decrease with decreasing values of $r_{\lambda,1}$, $r_{\lambda,2}$, $r_{\lambda,3}$ and $r_{\lambda,X}$ ($r_{\chi,X}$) in the parameter region considered. With fixed values of k' and $M_*/\pi k'$, the quantity $\delta\hat{m}_\varphi^2|_\lambda^{(1)}$ depends only on $r_{\lambda,i}$ and $r_{\lambda,X}$, $\delta\hat{m}_\varphi^2|_{\lambda,i}^{(2)}$ on $r_{\lambda,i}$ (with a tiny dependence on $r_{\lambda,X}$), and $\delta\hat{m}_\varphi^2|_\chi$ on $r_{\chi,X}$.
- The xyon mass scales almost linearly with k' .

- The scaling of the xyon mass with $M_*/\pi k'$ is not very simple, but they are positively correlated. (Note that $M_*/\pi k' \rightarrow \alpha(M_*/\pi k')$ with the other parameters fixed is equivalent to $r_{\lambda,i} \rightarrow \alpha r_{\lambda,i}$, $r_{\lambda,X} \rightarrow \alpha r_{\lambda,X}$ and $r_{\chi,X} \rightarrow \alpha^2 r_{\chi,X}$ with the other parameters fixed.)

These features are used in section 4.3 in the discussion of the xyon mass in the holographic 5D theories.

Appendix B

In this Appendix we present the propagators for the gauginos and gauge scalars, relevant for the calculation of the xyon mass.

B.1 Gaugino propagators

Here we present the propagators for the $U(1)_Y$, $SU(2)_L$, $SU(3)_C$ and XY gauginos. We present the propagators \hat{G} for the rescaled fields, $\hat{\lambda}_\alpha^A = e^{-2k|y|}\lambda_\alpha^A$ and $\hat{\lambda}'_\alpha{}^A = e^{-2k|y|}\lambda'^A_\alpha$. The propagators for the non-rescaled fields are given by $G = e^{2k(|y|+|y'|)}\hat{G}$.

The gaugino propagators take the form of 4×4 matrices in the space of $\{\hat{\lambda}_\alpha^A, \hat{\lambda}'^{\dagger\dot{\alpha}A}, \hat{\lambda}^{\dagger\dot{\alpha}A}, \hat{\lambda}'^A_\alpha\}$:

$$\hat{G}^S \equiv \left(\begin{array}{cc|cc} \hat{G}^S_{\lambda\lambda^\dagger}(z, z'; p)_{\alpha\dot{\beta}} & \hat{G}^S_{\lambda\lambda'}(z, z'; p)_\alpha^\beta & \hat{G}^S_{\lambda\lambda}(z, z'; p)_\alpha^\beta & \hat{G}^S_{\lambda\lambda^\dagger}(z, z'; p)_{\alpha\dot{\beta}} \\ \hat{G}^S_{\lambda^\dagger\lambda^\dagger}(z, z'; p)_{\dot{\alpha}\dot{\beta}} & \hat{G}^S_{\lambda^\dagger\lambda'}(z, z'; p)^{\dot{\alpha}\beta} & \hat{G}^S_{\lambda^\dagger\lambda}(z, z'; p)^{\dot{\alpha}\beta} & \hat{G}^S_{\lambda^\dagger\lambda^\dagger}(z, z'; p)_{\dot{\alpha}\dot{\beta}} \\ \hline \hat{G}^S_{\lambda^\dagger\lambda^\dagger}(z, z'; p)_{\dot{\alpha}\dot{\beta}} & \hat{G}^S_{\lambda^\dagger\lambda'}(z, z'; p)^{\dot{\alpha}\beta} & \hat{G}^S_{\lambda^\dagger\lambda}(z, z'; p)^{\dot{\alpha}\beta} & \hat{G}^S_{\lambda^\dagger\lambda^\dagger}(z, z'; p)_{\dot{\alpha}\dot{\beta}} \\ \hat{G}^S_{\lambda'\lambda^\dagger}(z, z'; p)_{\alpha\dot{\beta}} & \hat{G}^S_{\lambda'\lambda'}(z, z'; p)_\alpha^\beta & \hat{G}^S_{\lambda'\lambda}(z, z'; p)_\alpha^\beta & \hat{G}^S_{\lambda'\lambda^\dagger}(z, z'; p)_{\alpha\dot{\beta}} \end{array} \right), \quad (86)$$

where the superscript S takes either “321, i ” (with $i = 1, 2, 3$ for $U(1)_Y$, $SU(2)_L$ and $SU(3)_C$) or “XY” (for $SU(5)/321$). Here, we have given the propagators in the mixed position-momentum space: $z \equiv e^{k|y|}/k$ (and z') represents the coordinate for the fifth dimension and p the 4D momentum.

The propagators are written in the following form [32]:

$$\hat{G}^S = \left(\begin{array}{cc|cc} i\sigma_{\alpha\dot{\beta}}^\mu p_\mu f^S & i\delta_\alpha^\beta (-\partial_z + \frac{1}{2z}) f'^S & i\delta_\alpha^\beta h^S & \frac{i\sigma_{\alpha\dot{\beta}}^\mu p_\mu}{p^2} (\partial_z - \frac{1}{2z}) h'^S \\ i\delta_{\dot{\beta}}^{\dot{\alpha}} (\partial_z + \frac{1}{2z}) f^S & i\bar{\sigma}^{\mu\dot{\alpha}\beta} p_\mu f'^S & \frac{i\bar{\sigma}^{\mu\dot{\alpha}\beta} p_\mu}{p^2} (-\partial_z - \frac{1}{2z}) h^S & i\delta_{\dot{\beta}}^{\dot{\alpha}} h'^S \\ \hline i\delta_{\dot{\beta}}^{\dot{\alpha}} h^S & \frac{i\bar{\sigma}^{\mu\dot{\alpha}\beta} p_\mu}{p^2} (\partial_z - \frac{1}{2z}) h'^S & i\bar{\sigma}^{\mu\dot{\alpha}\beta} p_\mu f^S & i\delta_{\dot{\beta}}^{\dot{\alpha}} (-\partial_z + \frac{1}{2z}) f'^S \\ \frac{i\sigma_{\alpha\dot{\beta}}^\mu p_\mu}{p^2} (-\partial_z - \frac{1}{2z}) h^S & i\delta_\alpha^\beta h'^S & i\delta_\alpha^\beta (\partial_z + \frac{1}{2z}) f^S & i\sigma_{\alpha\dot{\beta}}^\mu p_\mu f'^S \end{array} \right). \quad (87)$$

Here, f^S , f'^S , h^S and h'^S are the functions of z , z' and p :

$$f^S(z, z'; p) = \frac{g_5^2 \sqrt{z < z'}}{(C^S - A^S)^2 + (B^S)^2} \left(I_1(|p|z <) + C^S K_1(|p|z <) \right)$$

$$\times \left((C^S - A^S) \left\{ I_1(|p|z_>) + A^S K_1(|p|z_>) \right\} - (B^S)^2 K_1(|p|z_>) \right), \quad (88)$$

$$f'^S(z, z'; p) = -\frac{g_5^2 \sqrt{z_< z_>}}{(C^S - A^S)^2 + (B^S)^2} \left(I_0(|p|z_<) - C^S K_0(|p|z_<) \right) \\ \times \left((C^S - A^S) \left\{ I_0(|p|z_>) - A^S K_0(|p|z_>) \right\} + (B^S)^2 K_0(|p|z_>) \right), \quad (89)$$

$$h^S(z, z'; p) = -\frac{g_5^2 |p| \sqrt{z_< z_>}}{(C^S - A^S)^2 + (B^S)^2} \left(I_1(|p|z_<) + C^S K_1(|p|z_<) \right) \\ \times B^S \left(I_1(|p|z_>) + C^S K_1(|p|z_>) \right), \quad (90)$$

$$h'^S(z, z'; p) = \frac{g_5^2 |p| \sqrt{z_< z_>}}{(C^S - A^S)^2 + (B^S)^2} \left(I_0(|p|z_<) - C^S K_0(|p|z_<) \right) \\ \times B^S \left(I_0(|p|z_>) - C^S K_0(|p|z_>) \right), \quad (91)$$

where $|p| \equiv \sqrt{p^2}$ and $z_< (z_>)$ is the lesser (greater) of z and z' .

The coefficients A^S , B^S and C^S are given by

$$A^S = \frac{X_I^S X_K^S - Y_I^S Y_K^S}{(X_K^S)^2 + (Y_K^S)^2}, \quad B^S = \frac{X_I^S Y_K^S + X_K^S Y_I^S}{(X_K^S)^2 + (Y_K^S)^2}, \quad C^S = \frac{Z_I^S}{Z_K^S}. \quad (92)$$

For the 321 gauginos ($S = 321, i$),

$$\left\{ \begin{array}{l} X_I^{321,i} = \frac{1}{g_5^2} I_0\left(\frac{|p|}{k'}\right), \\ X_K^{321,i} = \frac{1}{g_5^2} K_0\left(\frac{|p|}{k'}\right), \end{array} \right\} \quad \left\{ \begin{array}{l} Y_I^{321,i} = M_{\lambda,i} I_1\left(\frac{|p|}{k'}\right), \\ Y_K^{321,i} = M_{\lambda,i} K_1\left(\frac{|p|}{k'}\right), \end{array} \right\} \quad \left\{ \begin{array}{l} Z_I^{321,i} = \frac{1}{g_5^2} I_0\left(\frac{|p|}{k}\right) - \frac{|p|}{\tilde{g}_{0,i}^2} I_1\left(\frac{|p|}{k}\right), \\ Z_K^{321,i} = \frac{1}{g_5^2} K_0\left(\frac{|p|}{k}\right) + \frac{|p|}{\tilde{g}_{0,i}^2} K_1\left(\frac{|p|}{k}\right), \end{array} \right\} \quad (93)$$

where we have neglected the contributions from the IR-brane gauge kinetic terms (see the text).

For the XY gauginos ($S = XY$),

$$\left\{ \begin{array}{l} X_I^{XY} = \frac{1}{g_5^2} I_1\left(\frac{|p|}{k'}\right), \\ X_K^{XY} = -\frac{1}{g_5^2} K_1\left(\frac{|p|}{k'}\right), \end{array} \right\} \quad \left\{ \begin{array}{l} Y_I^{XY} = M_{\lambda,X} I_0\left(\frac{|p|}{k'}\right), \\ Y_K^{XY} = -M_{\lambda,X} K_0\left(\frac{|p|}{k'}\right), \end{array} \right\} \quad \left\{ \begin{array}{l} Z_I^{XY} = I_1\left(\frac{|p|}{k}\right), \\ Z_K^{XY} = -K_1\left(\frac{|p|}{k}\right). \end{array} \right\} \quad (94)$$

B.2 Gauge scalar propagators

Here we present the propagators for the gauge scalars, χ^{321} and χ^{XY} . For gauge scalars, differences among the $U(1)_Y$, $SU(2)_L$ and $SU(3)_C$ components are not important, as these fields are strongly localized towards the IR brane and do not feel logarithmically enhanced UV-brane terms. We again present the propagators \hat{G} for the rescaled fields, $\hat{\chi}^A = e^{-2k|y|} \chi^A$.

In the mixed position-momentum space, the propagators are given by

$$\hat{G}_{\chi\chi}^S(z, z'; p) = \frac{ig_5^2}{k} \frac{1}{D^S - E^S} \left(I_0(|p|z_<) + D^S K_0(|p|z_<) \right) \left(I_0(|p|z_>) + E^S K_0(|p|z_>) \right), \quad (95)$$

where the superscript S takes either 321 or XY. The coefficients D^S and E^S are given for χ^{321} by

$$D^{321} = -\frac{I_0\left(\frac{|p|}{k}\right)}{K_0\left(\frac{|p|}{k}\right)}, \quad E^{321} = -\frac{I_0\left(\frac{|p|}{k'}\right)}{K_0\left(\frac{|p|}{k'}\right)}, \quad (96)$$

and for χ^{XY} by

$$D^{XY} = \frac{I_1\left(\frac{|p|}{k}\right)}{K_1\left(\frac{|p|}{k}\right)}, \quad E^{XY} = \frac{\frac{|p|}{k'} I_1\left(\frac{|p|}{k'}\right) + \frac{g_5^2 M_{X,X}^2}{k} I_0\left(\frac{|p|}{k'}\right)}{\frac{|p|}{k'} K_1\left(\frac{|p|}{k'}\right) - \frac{g_5^2 M_{X,X}^2}{k} K_0\left(\frac{|p|}{k'}\right)}. \quad (97)$$

References

- [1] E. Witten, Nucl. Phys. B **188**, 513 (1981).
- [2] S. Dimopoulos and H. Georgi, Nucl. Phys. B **193**, 150 (1981); N. Sakai, Z. Phys. C **11**, 153 (1981); S. Dimopoulos, S. Raby and F. Wilczek, Phys. Rev. D **24**, 1681 (1981).
- [3] Y. Nomura, D. Tucker-Smith and B. Tweedie, Phys. Rev. D **71**, 075004 (2005) [arXiv:hep-ph/0403170].
- [4] Z. Chacko, Y. Nomura and D. Tucker-Smith, arXiv:hep-ph/0504095.
- [5] S. Eidelman *et al.* [Particle Data Group Collaboration], Phys. Lett. B **592**, 1 (2004).
- [6] See, e.g., P. H. Chankowski, J. R. Ellis, M. Olechowski and S. Pokorski, Nucl. Phys. B **544**, 39 (1999) [arXiv:hep-ph/9808275]; M. Bastero-Gil, G. L. Kane and S. F. King, Phys. Lett. B **474**, 103 (2000) [arXiv:hep-ph/9910506]; J. A. Casas, J. R. Espinosa and I. Hidalgo, JHEP **0401**, 008 (2004) [arXiv:hep-ph/0310137].
- [7] LEP Higgs Working Group Collaboration, arXiv:hep-ex/0107030.
- [8] See, e.g., M. Carena, M. Quiros and C. E. M. Wagner, Nucl. Phys. B **461**, 407 (1996) [arXiv:hep-ph/9508343]; H. E. Haber, R. Hempfling and A. H. Hoang, Z. Phys. C **75**, 539 (1997) [arXiv:hep-ph/9609331].
- [9] R. Barbieri and G. F. Giudice, Nucl. Phys. B **306**, 63 (1988).
- [10] M. Dine, A. E. Nelson and Y. Shirman, Phys. Rev. D **51**, 1362 (1995) [arXiv:hep-ph/9408384]; M. Dine, A. E. Nelson, Y. Nir and Y. Shirman, Phys. Rev. D **53**, 2658 (1996) [arXiv:hep-ph/9507378].
- [11] M. Masip, R. Munoz-Tapia and A. Pomarol, Phys. Rev. D **57**, 5340 (1998) [arXiv:hep-ph/9801437]; J. R. Espinosa and M. Quiros, Phys. Rev. Lett. **81**, 516 (1998) [arXiv:hep-ph/9804235].
- [12] R. Harnik, G. D. Kribs, D. T. Larson and H. Murayama, Phys. Rev. D **70**, 015002 (2004) [arXiv:hep-ph/0311349]; S. Chang, C. Kilic and R. Mahbubani, Phys. Rev. D **71**, 015003 (2005) [arXiv:hep-ph/0405267].
- [13] A. Birkedal, Z. Chacko and Y. Nomura, Phys. Rev. D **71**, 015006 (2005) [arXiv:hep-ph/0408329].
- [14] M. Cvetič, D. A. Demir, J. R. Espinosa, L. L. Everett and P. Langacker, Phys. Rev. D **56**, 2861 (1997) [Erratum-ibid. D **58**, 119905 (1998)] [arXiv:hep-ph/9703317].
- [15] P. Batra, A. Delgado, D. E. Kaplan and T. M. P. Tait, JHEP **0402**, 043 (2004) [arXiv:hep-ph/0309149]; A. Maloney, A. Pierce and J. G. Wacker, arXiv:hep-ph/0409127.

- [16] The LEP Collaborations, the LEP Electroweak Working Group, and the SLD Electroweak and Heavy Flavour Groups, arXiv:hep-ex/0312023, as updated on <http://lepewwg.web.cern.ch/LEPEWWG/Welcome.html>
- [17] M. Dine and W. Fischler, Phys. Lett. B **110**, 227 (1982); Nucl. Phys. B **204**, 346 (1982); L. Alvarez-Gaume, M. Claudson and M. B. Wise, Nucl. Phys. B **207**, 96 (1982); S. Dimopoulos and S. Raby, Nucl. Phys. B **219**, 479 (1983).
- [18] P. Azzi *et al.* [CDF Collaborattion], arXiv:hep-ex/0404010.
- [19] CDF Collaborattion, <http://www-cdf.fnal.gov/physics/new/top/top.html>
- [20] K. Agashe and M. Graesser, Nucl. Phys. B **507**, 3 (1997) [arXiv:hep-ph/9704206]; see also, S. P. Martin, Phys. Rev. D **55**, 3177 (1997) [arXiv:hep-ph/9608224].
- [21] L. J. Hall and Y. Nomura, *Phys. Rev.* **D64**, 055003 (2001) [arXiv:hep-ph/0103125]; Y. Kawamura, *Prog. Theor. Phys.* **105**, 999 (2001) [arXiv:hep-ph/0012125]; for a review, L. J. Hall and Y. Nomura, *Annals Phys.* **306**, 132 (2003) [arXiv:hep-ph/0212134].
- [22] Y. Nomura and D. Tucker-Smith, Nucl. Phys. B **698**, 92 (2004) [arXiv:hep-ph/0403171].
- [23] G. 't Hooft, Nucl. Phys. B **72**, 461 (1974); E. Witten, Nucl. Phys. B **160**, 57 (1979).
- [24] N. Arkani-Hamed, M. Porrati and L. Randall, JHEP **0108**, 017 (2001) [arXiv:hep-th/0012148]; R. Rattazzi and A. Zaffaroni, JHEP **0104**, 021 (2001) [arXiv:hep-th/0012248].
- [25] L. Randall and R. Sundrum, Phys. Rev. Lett. **83**, 3370 (1999) [arXiv:hep-ph/9905221].
- [26] Y. Nomura, arXiv:hep-ph/0410348.
- [27] W. D. Goldberger, Y. Nomura and D. R. Smith, Phys. Rev. D **67**, 075021 (2003) [arXiv:hep-ph/0209158].
- [28] A. Pomarol, Phys. Rev. Lett. **85**, 4004 (2000) [arXiv:hep-ph/0005293].
- [29] T. Gherghetta and A. Pomarol, Nucl. Phys. B **586**, 141 (2000) [arXiv:hep-ph/0003129].
- [30] A. Hebecker, Nucl. Phys. B **632**, 101 (2002) [arXiv:hep-ph/0112230]; see also, D. Marti and A. Pomarol, Phys. Rev. D **64**, 105025 (2001) [arXiv:hep-th/0106256].
- [31] Z. Chacko, M. A. Luty and E. Ponton, JHEP **0007**, 036 (2000) [arXiv:hep-ph/9909248]; see also, Y. Nomura, Phys. Rev. D **65**, 085036 (2002) [arXiv:hep-ph/0108170].
- [32] Y. Nomura and D. R. Smith, Phys. Rev. D **68**, 075003 (2003) [arXiv:hep-ph/0305214].
- [33] F. E. Close, *An Introduction to Quarks and Partons* (Academic Press, London, 1979).
- [34] K. Cheung and G. C. Cho, Phys. Rev. D **67**, 075003 (2003) [arXiv:hep-ph/0212063]; Phys. Rev. D **69**, 017702 (2004) [arXiv:hep-ph/0306068].

- [35] H. C. Cheng, J. L. Feng and N. Polonsky, Phys. Rev. D **56**, 6875 (1997) [arXiv:hep-ph/9706438]; E. Katz, L. Randall and S. f. Su, Nucl. Phys. B **536**, 3 (1998) [arXiv:hep-ph/9801416].
- [36] H. Baer, K. m. Cheung and J. F. Gunion, Phys. Rev. D **59**, 075002 (1999) [arXiv:hep-ph/9806361].
- [37] A. Arvanitaki, C. Davis, P. W. Graham, A. Pierce and J. G. Wacker, arXiv:hep-ph/0504210.
- [38] See, e.g., M. L. Perl, P. C. Kim, V. Halyo, E. R. Lee, I. T. Lee, D. Loomba and K. S. Lackner, Int. J. Mod. Phys. A **16**, 2137 (2001) [arXiv:hep-ex/0102033].
- [39] T. K. Hemmick *et al.*, Phys. Rev. D **41**, 2074 (1990); for heavier nuclei, see E. B. Norman, S. B. Gazes and D. A. Bennett, Phys. Rev. Lett. **58** (1987) 1403; W. J. Dick, G. W. Greenlees and S. L. Kaufman, Phys. Rev. D **33**, 32 (1986).
- [40] P. F. Smith, J. R. J. Bennett, G. J. Homer, J. D. Lewin, H. E. Walford and W. A. Smith, Nucl. Phys. B **206**, 333 (1982).
- [41] A. De Rujula, S. L. Glashow and U. Sarid, Nucl. Phys. B **333**, 173 (1990); S. Dimopoulos, D. Eichler, R. Esmailzadeh and G. D. Starkman, Phys. Rev. D **41**, 2388 (1990).
- [42] R. N. Mohapatra and S. Nussinov, Phys. Rev. D **57**, 1940 (1998) [arXiv:hep-ph/9708497].
- [43] G. D. Starkman, A. Gould, R. Esmailzadeh and S. Dimopoulos, Phys. Rev. D **41**, 3594 (1990).
- [44] R. N. Mohapatra and V. L. Teplitz, Phys. Rev. Lett. **81**, 3079 (1998) [arXiv:hep-ph/9804420].
- [45] D. Abrams *et al.* [CDMS Collaboration], Phys. Rev. D **66**, 122003 (2002) [arXiv:astro-ph/0203500]; D. S. Akerib *et al.* [CDMS Collaboration], Phys. Rev. D **68**, 082002 (2003) [arXiv:hep-ex/0306001].
- [46] S. Dimopoulos, G. F. Giudice and A. Pomarol, Phys. Lett. B **389**, 37 (1996) [arXiv:hep-ph/9607225].
- [47] F. Aharonian *et al.* [The HESS Collaboration], arXiv:astro-ph/0408145; K. Kosack *et al.* [The VERITAS Collaboration], Astrophys. J. **608**, L97 (2004) [arXiv:astro-ph/0403422].
- [48] D. Hooper and J. March-Russell, Phys. Lett. B **608**, 17 (2005) [arXiv:hep-ph/0412048]; M. Ibe, K. Tobe and T. Yanagida, arXiv:hep-ph/0503098.
- [49] M. Viel, J. Lesgourgues, M. G. Haehnelt, S. Matarrese and A. Riotto, Phys. Rev. D **71**, 063534 (2005) [arXiv:astro-ph/0501562].
- [50] P. Creminelli, A. Nicolis and R. Rattazzi, JHEP **0203**, 051 (2002) [arXiv:hep-th/0107141].

- [51] M. Fukugita and T. Yanagida, *Phys. Lett. B* **174**, 45 (1986); for a recent review, W. Buchmuller, R. D. Peccei and T. Yanagida, arXiv:hep-ph/0502169.
- [52] Y. Grossman, R. Kitano and H. Murayama, arXiv:hep-ph/0504160.
- [53] P. J. Fox, A. E. Nelson and N. Weiner, *JHEP* **0208**, 035 (2002) [arXiv:hep-ph/0206096].
- [54] Z. Chacko, P. J. Fox and H. Murayama, *Nucl. Phys. B* **706**, 53 (2005) [arXiv:hep-ph/0406142].